8-21-2022

Seasonality of precipitation in the southwestern United States during the late Pleistocene inferred from stable isotopes in herbivore tooth enamel

Matthew J. Kohn

Kathleen B. Springer

Jeffrey S. Pigati

Linda M. Reynard

Amanda E. Drewicz

See next page for additional authors

Authors

Matthew J. Kohn, Kathleen B. Springer, Jeffrey S. Pigati, Linda M. Reynard, Amanda E. Drewicz, Justin Crevier, and Eric Scott

Quaternary Science Reviews 296 (2022) 107784

Contents lists available at ScienceDirect

Quaternary Science Reviews

journal homepage: www.elsevier.com/locate/quascirev

Seasonality of precipitation in the southwestern United States during the late Pleistocene inferred from stable isotopes in herbivore tooth enamel

Matthew J. Kohn [a, *], Kathleen B. Springer [b], Jeffrey S. Pigati [b], Linda M. Reynard [a], Amanda E. Drewicz [a], Justin Crevier [a], Eric Scott [c, d]

[a] Department of Geosciences, Boise State University, 1910 University Dr., Boise, ID 83725, USA
[b] U.S. Geological Survey, Denver Federal Center, Box 25046, MS 980, Denver, CO 80225, USA
[c] Department of Biology, California State University, San Bernardino, CA 92407, USA
[d] Cogstone Resource Management, Inc., 1518 Taft Ave., Orange, CA 92865, USA

ARTICLE INFO

Article history:
Received 22 June 2022
Received in revised form
20 September 2022
Accepted 21 September 2022
Available online 12 October 2022

Handling Editor: Dr. I. Hendy

Keywords:
Late Pleistocene
Tooth enamel
Paleowetlands
Southwestern U.S.
Stable isotopes
Paleoclimate

ABSTRACT

The late Pleistocene was a climatically dynamic period, with abrupt shifts between cool-wet and warm-dry conditions. Increased effective precipitation supported large pluvial lakes and long-lived spring ecosystems in valleys and basins throughout the western and southwestern U.S., but the source and seasonality of the increased precipitation are debated. Increases in the proportions of $C_4/(C_4+ C_3)$ grasses in the diets of large grazers have been ascribed both to increases in summer precipitation and lower atmospheric CO_2 levels. Here we present stable carbon and oxygen isotope data from tooth enamel of late Pleistocene herbivores recovered from paleowetland deposits at Tule Spring Fossil Beds National Monument in the Las Vegas Valley of southern Nevada, as well as modern herbivores from the surrounding area. We use these data to investigate whether winter or summer precipitation was responsible for driving the relatively wet hydroclimate conditions that prevailed in the region during the late Pleistocene. We also evaluate whether late Pleistocene grass $C_4/(C_4+ C_3)$ was higher than today, and potential drivers of any changes.

Tooth enamel $\delta^{18}O$ values for Pleistocene *Equus*, *Bison*, and *Mammuthus* are generally low (average 22.0 ± 0.7‰, 2 s.e., VSMOW) compared to modern equids (27.8 ± 1.5‰), and imply lower water $\delta^{18}O$ values (−16.1 ± 0.8‰) than modern precipitation (−10.5‰) or in waters present in active springs and wells in the Las Vegas Valley (−12.9‰), an area dominated by winter precipitation. In contrast, tooth enamel of *Camelops* (a browser) generally yielded higher $\delta^{18}O$ values (23.9 ± 1.1‰), possibly suggesting drought tolerance. Mean $\delta^{13}C$ values for the Pleistocene grazers (−6.6 ± 0.7‰, 2 s.e., VPDB) are considerably higher than for modern equids (−9.6 ± 0.4‰) and indicate more consumption of C_4 grass (17 ± 5%) than today (4 ± 4%). However, calculated C_4 grass consumption in the late Pleistocene is strikingly lower than the proportion of C_4 grass taxa currently present in the valley (55–60%). $\delta^{13}C$ values in *Camelops* tooth enamel (−7.7 ± 1.0‰) are interpreted as reflecting moderate consumption (14 ± 8%) of *Atriplex* (saltbush), a C_4 shrub that flourishes in regions with hot, dry summers.

Lower water $\delta^{18}O$ values, lower abundance of C_4 grasses, and the inferred presence of *Atriplex* are all consistent with general circulation models for the late Pleistocene that show enhanced delivery of winter precipitation, sourced from the north Pacific, into the interior western U.S. but do not support alternative models that infer enhanced delivery of summer precipitation, sourced from the tropics. In addition, we hypothesize that dietary competition among the diverse and abundant Pleistocene fauna may have driven the grazers analyzed here to feed preferentially on C_4 grasses. Dietary partitioning, especially when combined with decreased p_{CO2} levels during the late Pleistocene, can explain the relatively high $\delta^{13}C$ values observed in late Pleistocene grazers in the Las Vegas Valley and elsewhere in the southwestern U.S. without requiring additional summer precipitation. Pleistocene hydroclimate parameters

* Corresponding author.
E-mail address: mattkohn@boisestate.edu (M.J. Kohn).

https://doi.org/10.1016/j.quascirev.2022.107784

derived from dietary and floral records may need to be reevaluated in the context of the potential effects of dietary preferences and lower p_{CO2} levels on the stability of C_3 vs. C_4 plants.

1. Introduction

During the late Pleistocene, the western and southwestern U.S. supported numerous large lakes (e.g., Russell, 1885; Gilbert, 1890; Blackwelder, 1931; Snyder et al., 1964; Mifflin and Wheat, 1979; Williams and Bedinger, 1983; Benson and Thompson, 1987; Reheis, 1999). The largest of these lakes, Lake Bonneville and Lake Lahontan, dwarfed their modern descendants (Great Salt Lake and Pyramid Lake) and lakes in smaller basins such as Death Valley (Lake Manly) no longer exist. Increased precipitation combined with lower temperatures and evaporation rates have long been inferred as the climate driver(s) that sustained these ancient water bodies (Broecker and Orr, 1958).

Although pluvial lakes in the western and southwestern U.S. are iconic late Pleistocene environments, extensive spring ecosystems were also widespread during the middle-late Pleistocene and early Holocene (e.g., Quade, 1986; Quade and Pratt, 1989; Quade et al., 1995, 1998, 2003; Pigati et al., 2009, 2011; Springer et al., 2015, 2018; Honke et al., 2019). The spatial distribution of springs and wetlands depends on topographically, structurally, hydrologically, and climatically interacting factors that combine to produce different spring hydrologic environments that wax and wane over time. However, for a given geographically and structurally defined system, increased spring discharge generally reflects an increase in effective precipitation in the adjacent mountain recharge areas (here, effective precipitation is considered to be precipitation minus evaporation and transpiration). Geologic deposits associated with springs and wetlands, therefore, can be used to infer changes in precipitation regimes on local to regional spatial scales.

The Las Vegas Formation represents one of the largest and best studied paleowetland depositional sequences on Earth. Located in the Las Vegas Valley of southern Nevada, the deposits of this formation have been the subject of detailed work spanning more than 50 years (Haynes, 1967; Quade, 1986; Quade and Pratt, 1989; Quade et al., 1995, 1998, 2003; Bell et al., 1998, 1999; Lundstrom et al., 1998; Page et al., 2005; Ramelli et al., 2011, 2012; Springer et al., 2015, 2018; Springer and Pigati, 2020; Goldstein et al., 2021), especially along the upper Las Vegas Wash within Tule Springs Fossil Beds National Monument (TUSK). The Las Vegas Formation consists of sequences of paleo-wetland deposits that represent distinct periods of high water tables and spring activity that were interrupted by dry periods characterized by erosion, desiccation, and/or soil formation. Although the entirety of the formation spans half a million years, it is most highly resolved between ~40 and 8.5 ka where nearly 100 high-precision ^{14}C ages document the repeated expansion and contraction of wetlands in the Las Vegas Valley in response to millennial and submillennial-scale climate perturbations (Springer et al., 2015, 2018; Springer and Pigati, 2020). Of interest to this study, abundant fossils of large herbivores from the Tule Springs local fauna (Scott et al., 2017), which were entombed in the sediments of the Las Vegas Formation, permit investigation of stable isotope compositions from tooth enamel of the various taxa. These data can be linked to water compositions and paleoecology to test hypotheses regarding past climatic drivers.

Why was the western U.S. wetter during the late Pleistocene? Although lower temperatures must have decreased evaporation and therefore increased effective precipitation, models of lake levels indicate that an increase in absolute annual precipitation is also required (e.g., Hostetler and Benson, 1990). If so, where did the additional moisture come from? Two hypotheses are currently debated. Many general circulation models (GCMs) predict a southward "Shift Of the Westerlies" (SOW model), which increased seasonal proportions of winter precipitation sourced from the northern and eastern Pacific (e.g., COHMAP Members, 1988; Toggweiler et al., 2006; Kim et al., 2008; Alder and Hostetler, 2015; Fig. 1A). These models predict the Cordilleran and Laurentide ice sheets split the jet stream into a weak northward (sub)stream and a much stronger southward (sub)stream. The southern jet stream would have delivered winter (but not summer) storms inland efficiently to the Great Basin and southwestern U.S., aiding in the expansions of Pleistocene lakes and wetlands (Fig. 1A). In contrast, Lyle et al. (2012) proposed that increased late Pleistocene precipitation in the southwestern U.S. resulted from enhanced summer (but not winter) precipitation sourced "Out Of the Tropics" (OOT model) from the Pacific Ocean and/or Gulf of Mexico (Fig. 1B).

Although we do not know of any GCMs that independently predict OOT precipitation for the southwestern U.S. during the late Pleistocene, seasonal differences in moisture delivery would have influenced $\delta^{18}O$ values of precipitation and the proportions of grass functional groups (C_3 vs. C_4 grasses). For reasons discussed in Section 4, enhanced winter precipitation and lower temperatures should cause a decrease in both precipitation $\delta^{18}O$ and $C_4/(C_4 + C_3)$, whereas enhanced summer precipitation should cause an increase in both precipitation $\delta^{18}O$ and $C_4/(C_4 + C_3)$. For example, winter vs. summer precipitation in southern Nevada today derives from high vs. low latitudes and has mean $\delta^{18}O$ values of −12.3 vs. −4.7‰, respectively (Lachniet et al., 2020). Because $\delta^{18}O$ and $\delta^{13}C$ values of tooth enamel in many large herbivores track local water composition and $C_4/(C_4 + C_3)$ (e.g., Koch, 1998, 2007; MacFadden, 2000; Kohn and Cerling, 2002; Kohn and Dettman, 2007; Clementz, 2012), measurement of $\delta^{18}O$ and $\delta^{13}C$ in tooth enamel from late Pleistocene herbivores in the western U.S. may allow us to discriminate between the OOT and SOW models.

In this study, we measured stable isotope compositions of carbon ($\delta^{13}C$ values) and oxygen ($\delta^{18}O$ values) of fossil herbivore tooth enamel of specimens from the Tule Springs local fauna, which were then combined with previously published enamel isotope data from the region. We focused especially on large mammals – *Equus*, *Bison*, *Mammuthus*, and *Camelops* – because their teeth are abundant and readily analyzed, their physiologies and diets are generally well known (which aids in interpreting isotope compositions), and their tooth enamel is resistant to diagenetic alteration (e.g., Kohn and Cerling, 2002). These data provide tests of the competing hypotheses regarding the source of increased precipitation that triggered paleowetland expansion in the Las Vegas Valley during the late Pleistocene.

2. The Las Vegas Formation

During the late Pleistocene, springs and wetlands covered at least ~1425 km^2 of the Las Vegas Valley in southern Nevada, USA (Harrill, 1976). Distinctive, light-colored sediments associated with these ecosystems are called the Las Vegas Formation (Longwell

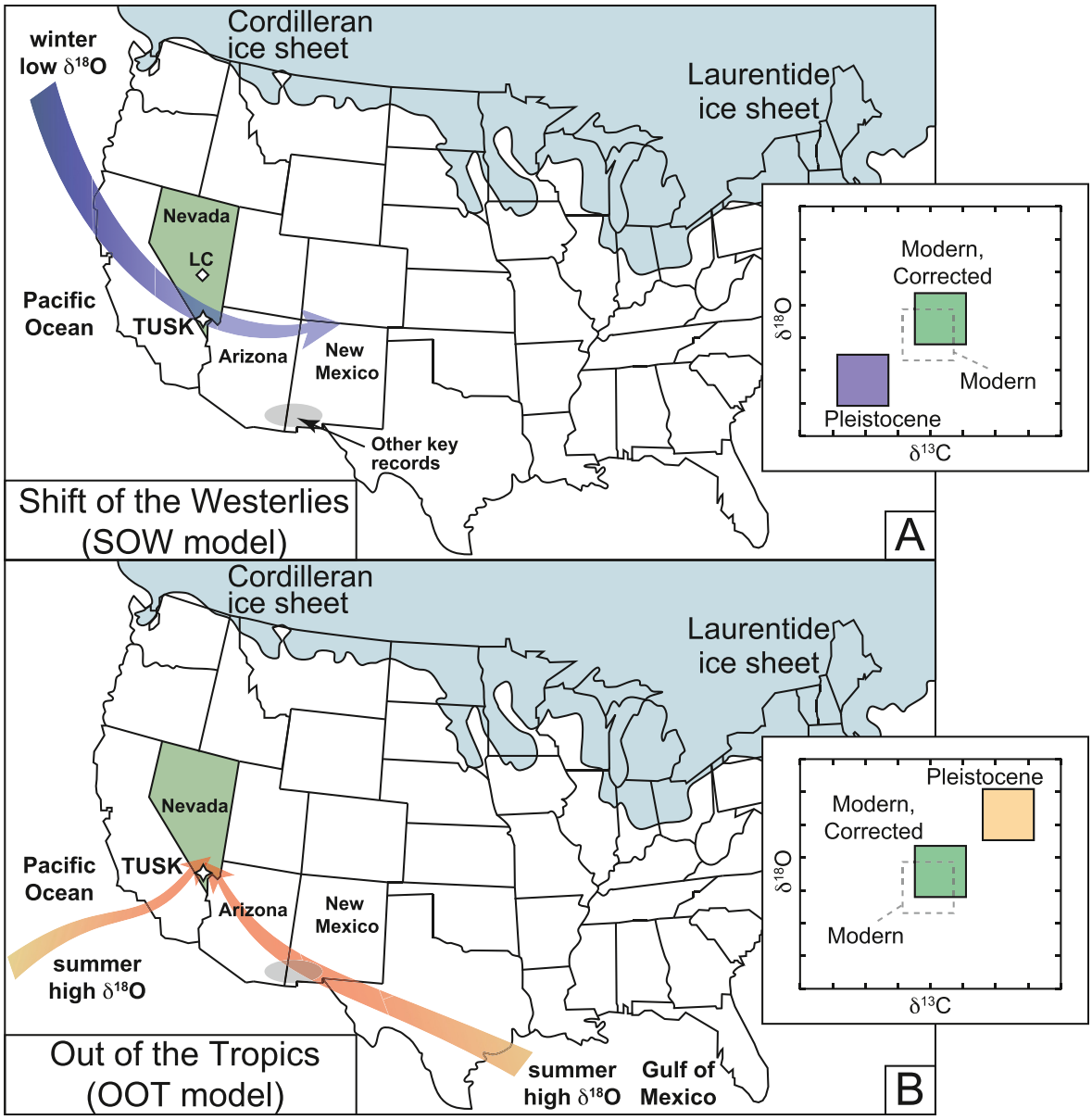

Fig. 1. Location map of Tule Springs Fossil Beds National Monument in the upper Las Vegas Wash study area (white star labeled TUSK) in southern Nevada, and different modes of moisture sources. Insets show isotopic expectations of different models; secular changes to $\delta^{13}C$ and $\delta^{18}O$ values are needed to compare modern and Pleistocene compositions. Gray oval shows region in southern Arizona and New Mexico with strongest evidence for summer precipitation during the late Pleistocene. LC = Leviathan Cave. (A) Enhanced winter precipitation from a southward shift of the westerlies (SOW; COHMAP, 1988) should decrease $\delta^{13}C$ values (fewer C_4 grasses) and $\delta^{18}O$ values (colder, northern moisture source during winter). (B) Enhanced summer precipitation from moisture derived out of the tropics (OOT; Lyle et al., 2012) should increase $\delta^{13}C$ values (more C_4 grasses) and $\delta^{18}O$ values (warmer, southern moisture source during summer). Continental ice sheet extent is for 18 ^{14}C ka (Dalton et al., 2020); glaciations in Rocky, Cascade, and Sierra Nevada Mountains were omitted for simplicity.

et al., 1965). Haynes (1967) subdivided the formation into informal stratigraphic units A-E (oldest to youngest), with some strata further subdivided (e.g., E_1, E_2, etc.). With the aid of numerous new stratigraphic section measurements and a suite of radiocarbon and luminescence ages, Springer et al. (2018) made detailed descriptions of the different strata, interpreted the depositional and spring hydrologic environments recorded in the sediments, and correlated the paleohydrologic regimes with independent climate records. They recognize members X, A, B, D, E (oldest to youngest) and further subdivide members B, D, and E into their attendant beds (Fig. 2A). Vertebrate fossils comprising the Tule Springs local fauna include abundant megafauna, dominated by remains of *Mammuthus* and *Camelops*, along with less common remains of *Equus* and *Bison* (Mawby, 1967; Scott et al., 2017). Remains of these taxa are present in members B, D, and E (Scott et al., 2017), and date to between ~100 and 12.5 ka (Springer et al., 2018). The descriptions of the fossil-bearing strata below follow Springer et al. (2018). Luminescence ages in this discussion are also from Springer et al. (2018), whereas calibrated ^{14}C ages are based on data reported in both Springer et al. (2018) and Springer and Pigati (2020) and recalibrated here using the IntCal20 dataset (Reimer et al., 2020).

Bed B_1 is the oldest unit of the Las Vegas Formation that contains vertebrate fossils and reflects multiple fluvial throughflow and wetting-drying events that took place between ~100 and 50 ka. In a few areas, laterally discontinuous, cauldron-shaped bedforms of

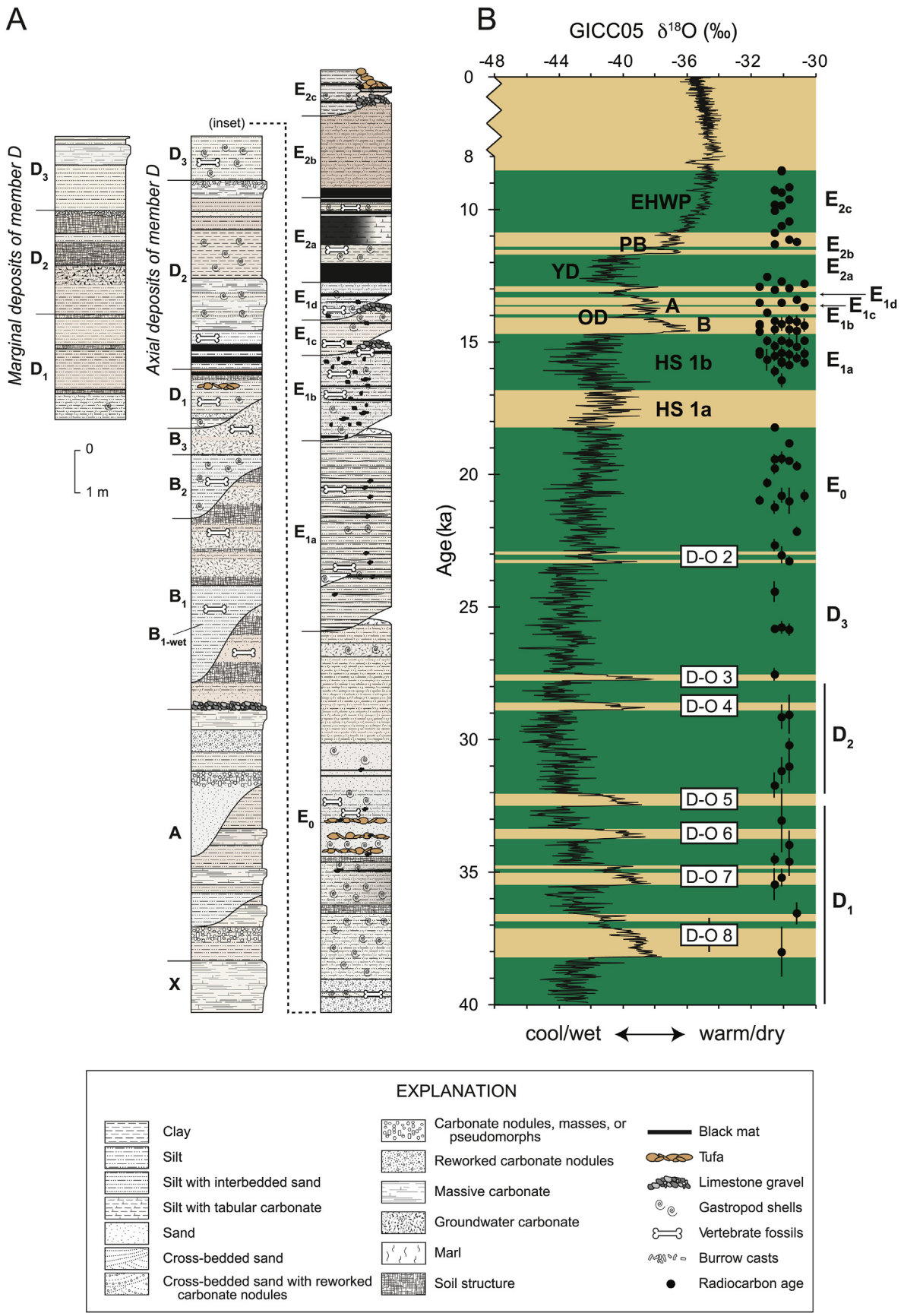

Fig. 2. (A) Composite stratigraphy for sediments of the Las Vegas Formation (after Springer et al., 2018). (B) Hydrologic record of members D and E (after Springer et al., 2018) compared to the timing of changes in oxygen isotope ($\delta^{18}O$) data from Greenland ice core records using the GICC05 chronology (Andersen et al., 2006). Periods of groundwater

pale green to gray clay, silt, and sand that are highly fossiliferous are inset within the deposits of bed B_1. This inset unit is referred to as bed $B_{1\text{-wet}}$ and represents spring-fed ponds that date to 72 ± 8 ka. Bed B_2 also represents spring-fed ponds and is highly fossiliferous. Luminescence ages for this bed range between 48 ± 4 and 47 ± 4 ka, whereas calibrated ^{14}C ages are 50.9 ± 4.1 and 50.4 ± 4.6 ka. Together, these dates imply an age range of ~55 to 45 ka for bed B_2. Bed B_3 is similar to bed B_1 and reflects fluvial channel and overbank deposits interrupted by brief periods of spring discharge, This bed dates to between ~45 and 40 ka.

Bed D_1 ranges in age from 38.0 ± 1.0 to 33.1 ± 1.2 ka and formed during large fluctuations in groundwater levels represented by pond and marsh environments, fluvial throughflow, and desiccation. Bed D_2 ranges in age from 31.7 ± 0.5 to 27.6 ± 0.2 ka. Axial deposits of this bed represent expansive marshes (green muds and sands) that grade towards valley margins, where drier conditions and phreatophyte flats (tan silts and sands) dominated the landscape. Bed D_3 also represents extensive marshes and marks the highest groundwater levels achieved in the Las Vegas Valley, which occurred between 25.9 ± 0.2 and 24.4 ± 0.4 ka, during the Last Glacial Maximum.

Member E is highly fossiliferous and is incised into older strata. Spring outflow stream deposits predominate, with minor pond and wet meadow deposits. Unlike older strata, the deposits of member E contain microbially mediated precipitates of tufa, which indicate rising temperatures crossed an unspecified threshold at this time. Bed E_0 formed during the latter part of the Last Glacial Maximum between 23.3 ± 0.2 and 18.2 ± 0.1 ka. Bed E_1 ranges in age from 16.1 ± 0.2 to 13.4 ± 0.1 ka and is further subdivided into four discrete depositional intervals that all formed during wet periods at 16.1 ± 0.2 to 15.0 ± 0.2 ka (bed E_{1a}), 14.6 ± 0.5 to 14.2 ± 0.2 ka (bed E_{1b}), 14.2 ± 0.2 to 13.9 ± 0.1 ka (bed E_{1c}), and 13.7 ± 0.1 to 13.4 ± 0.1 ka (bed E_{1d}). Bed E_2 represents discharge intervals during the Younger Dryas climate event (bed E_{2a}), preboreal oscillation (bed E_{2b}), and early Holocene (bed E_{2c}).

The detailed chronostratigraphy of the Las Vegas Formation, especially for members D and E, demonstrates abrupt hydrologic shifts from wet to dry conditions occurred on time scales of as little as a century. The close temporal correspondence between wetland expansion and contraction with the cool-warm periods recorded in Greenland ice cores (Andersen et al., 2006), as well as the close correlation between arid intervals that interrupted full glacial marshes of member D and Dansgaard-Oeschger abrupt warming events (Fig. 2B), demonstrates strong teleconnections existed between the North Atlantic and mid-latitude climates in North America during the late Pleistocene (Springer et al., 2015). Vertebrate fossils are concentrated in the paleowetland deposits, so the data presented here illuminate processes occurring when moisture to the southwestern U.S. was enhanced.

3. Stable isotope geochemistry of tooth enamel

The mineral component of teeth consists of hydroxylapatite with major substitutions of CO_3 for PO_4 and OH groups. Enamel is commonly selected for stable isotope analysis because it is resistant to diagenetic alteration, and therefore it preserves biogenic isotope compositions (e.g., Kohn and Cerling, 2002). Tooth enamel stable carbon and oxygen isotope compositions capture a record of ecological and climatic conditions, and are commonly used to reconstruct paleoclimate and paleoecology (see reviews by Koch, 1998, 2007; Kohn and Cerling, 2002; Clementz, 2012). Because teeth grow progressively, tooth enamel can also record sub-annual isotopic variations that in turn reflect sub-annual variations in climate and diet (Fricke and O'Neil, 1996; Fricke et al., 1998; Kohn et al., 1998). In general, tooth enamel is preferred for analysis because it is highly resistant to diagenetic alteration, both physically (Ayliffe et al., 1994) and isotopically (see summary of Kohn and Cerling, 2002). The preservation of systematic isotopic zoning in Pleistocene teeth observed in this study and many other studies (e.g., Kohn et al., 2005; Vetter, 2007; DeSantis et al., 2009; Feranec et al., 2009; Biasatti et al., 2010; Kohn and McKay, 2012; Trayler et al., 2015; Yann et al., 2016; etc.) further suggests that post-burial isotopic alteration of sub-fossil teeth must be small.

3.1. Oxygen isotopes in tooth enamel

Isotope compositions in water, plants, and animals vary on both intra-annual and longer timescales. Oxygen isotope compositions broadly correlate with hydrology and reflect precipitation sources and regional climate, as well as changes in temperature and evaporation. In general, low $\delta^{18}O$ values reflect cooler-wetter conditions, whereas higher $\delta^{18}O$ values reflect warmer-drier conditions. Oxygen isotope compositions in the tooth enamel of water-dependent herbivores strongly correlate with local water compositions (Kohn, 1996; Kohn and Cerling, 2002). The slope of a regression line correlating tooth enamel $\delta^{18}O$ with local water $\delta^{18}O$ is generally less than 1.0 (typically ~0.9) because animals derive a small fraction of intake oxygen from isotopically invariant sources, especially atmospheric O_2 (Kohn, 1996). Consequently, a shift in water-dependent herbivore $\delta^{18}O$ implies a slightly larger change in local water $\delta^{18}O$. One reason we chose to analyze *Bison*, *Mammuthus*, and *Equus* is because modern tooth $\delta^{18}O$ values for nearest living relatives (Bovinae including *Bison*, Elephantidae, and *Equus*, respectively) closely correlate with local water $\delta^{18}O$ (e.g., Kohn and Cerling, 2002).

Physiology can also affect oxygen isotope compositions, and drought-tolerant herbivores typically have higher $\delta^{18}O$ values than water-dependent animals, reflecting water-conserving adaptations (Ayliffe and Chivas, 1990; Luz et al., 1990). Correlation between $\delta^{18}O$ of drought-tolerant animals and local precipitation can be quite poor (e.g., Kohn and Cerling, 2002), so $\delta^{18}O$ of drought-tolerant mammals is not generally used to infer changes to local water $\delta^{18}O$. Our analysis included *Camelops*, and although the drought tolerance of this taxon is not well understood, modern large camels are highly drought-tolerant (e.g., Schmidt-Nielsen et al., 1956). Consequently, the *Camelops* $\delta^{18}O$ data were not used to infer changes to local water $\delta^{18}O$ values.

3.2. Carbon isotopes in tooth enamel

Carbon isotope compositions of herbivores depend on the isotope compositions of the plants they consume (DeNiro and Epstein, 1978). Different plants use different photosynthetic pathways - primarily C_3 or C_4 - with relatively high $\delta^{13}C$ values for C_4 plants (between −13 and −11‰ for modern plants; all carbon isotope compositions in this paper are presented relative to VPDB) and low $\delta^{13}C$ values for C_3 plants. While modern $\delta^{13}C$ values for most C_3 plants range between −32 and −23‰ (−28.5‰ for global

discharge are shown in green; periods of aridity are presented in tan. Dark filled circles are calibrated radiocarbon ages with uncertainties presented at the 95 percent (2σ) confidence level; data are from Springer et al. (2015, 2018) and Springer and Pigati (2020) and were recalibrated here using the IntCal20 dataset (Reimer et al., 2020). Millennial and submillennial scale climate events recorded in the sediments of the Las Vegas Formation include, from oldest to youngest, Dansgaard-Oeschger events (D–O), Heinrich interstadial (HS) 1a and stadial HS 1b, Bølling (B), Older Dryas (OD), Allerød (A), Younger Dryas (YD), pre-boreal oscillation (PB), and the early Holocene wet period (EHWP). (For interpretation of the references to color in this figure legend, the reader is referred to the Web version of this article.)

mean C_3 biomass), values in dry ecosystems are more typically −26 to −24‰ (Diefendorf et al., 2010; Kohn, 2010). C_4 plants are dominated by warm climate grasses and sedges that require high temperatures, significant warm-season precipitation, and high light levels in open habitats. In contrast, C_3 plants are represented by trees, shrubs, herbs, and cool-climate grasses. The isotopic offsets between tooth enamel and diet (plants) are known for many large herbivores (e.g., Cerling and Harris, 1999; Passey et al., 2005; Tejada-Lara et al., 2018), so tooth enamel compositions can be converted to effective plant compositions, which can then be used to infer plant ecology (e.g., abundance of isotopically distinct C_3 and C_4 plants). Herbivores commonly grade between end-member grazers (consumers of grass) and browsers (consumers of trees, shrubs, and herbs); mixed feeders are herbivores with intermediate graze-browse diets. To interpret tooth enamel isotope data, we must consider climatic controls on C_3 vs. C_4 grasses, and on different types of browse.

Open environments with warm and wet summers favor growth of C_4 grasses that confer high $\delta^{13}C$ values to grazer tooth enamel (e.g., Koch, 1998; MacFadden, 2000; Kohn and Cerling, 2002; Clementz, 2012). In contrast, environments with cool or dry summers favor growth of C_3 grasses that confer low $\delta^{13}C$ values to grazer tooth enamel (e.g., e.g., Koch, 1998; MacFadden, 2000; Kohn and Cerling, 2002; Clementz, 2012). Thus, analysis of grazer tooth enamel can indicate proportions of C_3 to C_4 grasses (e.g., MacFadden, 2000) and consequently changes to proportions of summer precipitation or temperature (e.g., Paruelo and Lauenroth, 1996). One reason we chose to analyze grazers (*Bison*, *Mammuthus*, and *Equus*) is because their $\delta^{13}C$ values should reflect the relative abundances of C_3 vs. C_4 grasses. Although grazers do consume other plant types, such as herbs and shrubs, the proportion of these plants in diet is typically less than 10–20% (e.g., van Vuren, 1984; Scasta et al., 2016).

Nearly all trees, shrubs, and herbs use the C_3 photosynthetic pathway. Consequently, in areas that have C_4 grasses, browsers commonly have low $\delta^{13}C$ values relative to grazers, and provide no information on abundances of C_3 vs. C_4 grasses. A nearly unique exception to the rule that C_4 plants are grasses or sedges, however, is that many species of the shrub saltbush (Amaranthaceae, *Atriplex* sp.) use C_4 photosynthesis. *Atriplex* is a minor but widespread plant in the western and southwestern interior of the United States, where summers typically have high daytime temperatures but very little precipitation. Many herbivores avoid saltbush because of its high salt content (hence the common name), but modern camels consume *Atriplex* preferentially (Towhidi et al., 2011). Consequently, although modern camels and the extinct taxon that we analyzed (*Camelops*) are browsers (Iqbal and Khan, 2001; Semprebon and Rivals, 2010; Yann et al., 2016), in areas where *Atriplex* is relatively common, camels should have elevated $\delta^{13}C$ values (Vetter, 2007), even if C_4 grasses are absent. Our analysis of *Camelops* therefore allows us to identify whether saltbush was a major component of its diet.

Tooth enamel is enriched in ^{13}C compared to consumed vegetation, so a conversion from tooth enamel $\delta^{13}C$ is required to infer local plant compositions. This is calculated via an enrichment factor, ε*, given by:

$$\varepsilon^* = \frac{\delta^{13}C_{tooth\ enamel} - \delta^{13}C_{diet}}{1 + \delta^{13}C_{diet/1000}} \quad (1)$$

Values of ε* increase with increasing body mass (Tejada-Lara et al., 2018) and reach 13.5 ± 1 to 14.5 ± 1‰ for large-bodied mammals, including equids/horses, bovids/bison and proboscideans (Cerling and Harris, 1999; Passey et al., 2005). Perissodactyls (*Equus* in this study) have long been viewed as exhibiting a lower ε* compared to artiodactyls (*Bison* and *Camelops*) because of differences in digestive methane production (Cerling and Harris, 1999). However, a recent review of enrichment factors for equids (Harris et al., 2020) indicates ε* = 14.5 ± 1, which is indistinguishable from bovines and elephants (Tejada-Lara et al., 2018). Camels may have a lower enrichment factor, ~13.7 ± 1‰ (Cerling and Harris, 1999). We use these values (ε* = 14.5 ± 1 for *Equus*, *Bison*, and *Mammuthus*; ε* = 13.7 ± 1 for *Camelops*) to infer $\delta^{13}C$ of herbivore diets from tooth enamel.

4. Implications of the SOW and OOT models for tooth enamel geochemistry

As discussed in Section 1, the SOW vs. OOT models imply different proportions of winter vs. summer precipitation, which should change ecosystem $\delta^{18}O$ values, the proportions of C_3 and C_4 grasses, and possibly the abundance of *Atriplex*. These expectations lead to specific predictions regarding tooth enamel isotope compositions (Fig. 1 insets).

Because lower-temperature winter precipitation has lower $\delta^{18}O$ values than higher-temperature summer precipitation (e.g., Dansgaard, 1964; Rozanski et al., 1993; Gat, 1996), an increase in the proportion of winter precipitation (SOW model) should result in a decrease in the $\delta^{18}O$ of mean annual precipitation. Conversely, an increase in the proportion of summer precipitation (OOT model) implies an increase in the $\delta^{18}O$ of mean annual precipitation. These changes of precipitation $\delta^{18}O$ should impart comparable changes to the $\delta^{18}O$ of plants and local water sources and be encoded in tooth enamel $\delta^{18}O$ of water-dependent herbivores – *Bison*, *Mammuthus*, and *Equus*. That is, relatively low $\delta^{18}O$ for these taxa (relative to modern) would support the SOW model (Fig. 1A), whereas relatively high $\delta^{18}O$ would support the OOT model (Fig. 1B).

The proportion of summer vs. winter precipitation also strongly influences the proportions of C_4 vs. C_3 grasses available to grazers (Paruelo and Lauenroth, 1996). An increase in winter precipitation (SOW) should decrease $C_4/(C_4 + C_3)$ and impart lower $\delta^{13}C$ values in grazers – *Bison*, *Mammuthus*, and *Equus* (Fig. 1A). In contrast, an increase in summer precipitation (OOT) should increase $C_4/(C_4 + C_3)$ relative to today and impart higher $\delta^{13}C$ values (Fig. 1B). Although we do not have an isotopic baseline for correlating $\delta^{13}C$ values in camels with *Atriplex* abundance, *Atriplex* favors dry summers. Consequently, very high $\delta^{13}C$ values in *Camelops* might favor the SOW model, whereas very low $\delta^{13}C$ values might favor the OOT model.

Seasonal isotope patterns might also help resolve SOW vs. OOT models. Because the OOT model enhances warm summer precipitation and associated C_4 grass abundance, grazers might be expected to show clear correlations between high $\delta^{18}O$ and high $\delta^{13}C$. Such patterns are commonly, albeit not ubiquitously, observed in latest Pleistocene (~13.0 ka) mammoth teeth from southeastern Arizona (Metcalfe et al., 2011), which today is strongly influenced by the North American monsoon.

5. Methods

5.1. Specimens

Thirty-nine fossil teeth were analyzed in this study, with most effort focused on the younger, more precisely dated beds E_0 and E_1 (26 teeth), but also including older beds B_1, B_2, D_1, and D_2 (13 teeth). Specifically, we analyzed a single *Bison* tooth from bed B_1; 6 teeth of *Bison* and *Equus* from bed B_2; 4 teeth of *Mammuthus*, *Equus,* and *Bison* from bed D_1; 2 teeth of *Mammuthus* from bed D_2; 13 teeth of *Camelops*, *Equus*, *Mammuthus*, and *Bison* from bed E_0; 3 teeth of

Equus and *Camelops* from bed E_{1a}; 7 teeth from *Mammuthus* and *Camelops* from bed E_{1b}; and 3 *Equus* teeth from bed E_{1d} (Fig. 2; Table 1). To provide an isotopic baseline for comparison, we also analyzed 9 teeth of modern feral horse (*Equus caballus*) from the Red Rock Herd Management Area (HMA), ~30 km west of Las Vegas (Table 1). Because we understand the diets and water-dependencies of *Mammuthus*, *Equus*, and *Bison* the best, and because we have modern data for *Equus*, our interpretations of isotopic data emphasize these taxa. We also analyzed *Camelops*, a browsing camelid that was slightly larger than modern camels, primarily to evaluate changes in abundance to the C_4 shrub, *Atriplex* (Vetter, 2007; Semprebon and Rivals, 2010). *Camelops* compositions also permit comparisons to the large grazers to support future work on diets and physiologies of extinct camelids. Interpretations include previously published data from Connin et al. (1998), representing 17 teeth of these same taxa from bed B_2 (2 *Bison*, 1 *Mammuthus*, 1 *Equus*), member D (undifferentiated; 1 *Mammuthus*, 1 *Equus*), and bed E_1 (undifferentiated; 5 *Mammuthus*, 3 *Equus*, 3 *Camelops*). We do not include data from Vetter (2007) because the fossils were not stratigraphically or chronologically well constrained.

5.2. Analytical methods

Enamel slices were cut along the length of each tooth, with a typical length of 20–70 mm, and subsampled every 1–2 mm, using a slow-speed microsaw. This approach retrieves sub-annual isotope variations while preserving tooth mineralization geometry (Trayler and Kohn, 2017), in contrast with an earlier investigation (Connin et al., 1998) that presented data representing a single bulk analyses per tooth. Fossil enamel was purified by separating it from dentine and grinding to a fine powder in a mortar and pestle. Powders were chemically cleaned at room temperature with 30% H_2O_2 and a 1 M acetic acid-Ca acetate buffer at 0.04 ml/mg to remove organic material and diagenetic carbonate respectively (Koch et al., 1997). Samples were rinsed 3–4 times in distilled-deionized water after each pretreatment step.

Powdered enamel (1.5–2.0 mg) was dissolved in supersaturated H_3PO_4 in a GasBench II, in-line with a Thermo Delta V Plus mass spectrometer, housed in the Stable Isotope Laboratory at Boise State University. Five to six aliquots of NIST-120c and an intralaboratory fossil bone standard ("KBS") were prepared using the same cleaning techniques and pre-treatment methods and analyzed with each sample set to assess analytical reproducibility and monitor for any sample preparation problems (none were observed). Eight to nine NBS-18 ($\delta^{13}C = -5.014$‰ VPDB and $\delta^{18}O = -23.2$‰ VPDB) and NBS-19 ($\delta^{13}C = +1.95$‰ VPDB and $\delta^{18}O = -2.2$‰ VPDB) calcite standards were also analyzed with each sample set for calibration to VPDB and VSMOW. Analytical reproducibility (2σ) for oxygen isotopes was: NIST = ±0.7‰; KBS = ±0.8‰; NBS-18 = ±0.6‰; and NBS-19 = ±0.6‰. For carbon isotopes, reproducibility (2σ) was ±0.3‰ for all materials. All further $\delta^{13}C$ and $\delta^{18}O$ values are reported to VPDB and VSMOW, respectively, except for $\delta^{18}O$ values for speleothem calcite from Leviathan Cave (Lachniet et al., 2014, 2017, 2020), which are reported to VPDB. Average $\delta^{13}C$ and $\delta^{18}O$ for NIST-120c were −6.4‰ and 28.8‰ respectively.

5.3. Secular corrections for isotope comparisons

Other than patterns of isotopic zoning, all comparisons between modern and fossil isotope compositions require corrections for secular changes to $\delta^{18}O$ and $\delta^{13}C$. These offsets are important for quantifying the magnitude of isotopic shifts associated with ecosystem and climate change, as well as for calculating grass $C_4/(C_4 + C_3)$. For oxygen isotopes, modern $\delta^{18}O$ values of the ocean and consequently the hydrologic cycle are ~1‰ lower than for the late Pleistocene because of changes to ice volume (Waelbroeck et al., 2002). Because all fossils predate major deglaciation of the latest Pleistocene, we adopt a 1‰ offset for our $\delta^{18}O$ data. For carbon isotopes, modern atmospheric $\delta^{13}C$ values are 1.3–1.6‰ lower than Pleistocene $\delta^{13}C$ values, mainly because of fossil fuel burning (Francey et al., 1999; Graven et al., 2017). For calculations requiring atmospheric $\delta^{13}C$ corrections, we use the time-resolved record of Eggleston et al. (2016), which covers the entire age range of interest. Calculations are referenced to a "modern" (AD 2000) atmospheric $\delta^{13}C$ value of −8.0‰.

5.4. Inferred water $\delta^{18}O$ values

Stable oxygen isotope compositions of tooth enamel were converted to equivalent $\delta^{18}O$ values of water ($\delta^{18}O_{water}$) to compare with modern water compositions and to evaluate any secular changes to water $\delta^{18}O$ values. Although $\delta^{18}O_{water}$ values may be estimated in principle from global correlations between $\delta^{18}O$ values for equids, bovines, and proboscideans vs. local $\delta^{18}O_{water}$ values (Kohn and Dettman, 2007; Kohn and Fremd, 2007), Hoppe et al. (2004) showed that large errors can accompany such estimates for horses in the western U.S interior. Commonly, correlations are calculated based on tooth enamel or bone $\delta^{18}O$ vs. precipitation $\delta^{18}O$. However, local water and food sources can be ^{18}O-enriched because of evaporation in extremely arid environments (e.g., Ayliffe and Chivas, 1990; Luz et al., 1990; Kohn, 1996; Levin et al., 2006). Thus, whereas the slope of a global correlation may be robust (because it reflects an animal's water balance, which is physiologically controlled; see Kohn, 1996), local tooth compositions can deviate from global trends (see Kohn and Dettman, 2007; Kohn and Fremd, 2007).

To overcome this problem, we fit an equation of the form $\delta^{18}O_{local\ water} = m \cdot \delta^{18}O_{tooth\ enamel} + b$ (where empirically-derived m = slope and b = constant intercept) that simultaneously accounts for global systematics in oxygen isotope compositions, physiologies of water-dependent taxa, and local compositions in Nevada. Key to this calibration are data for feral horses in Nevada (Crowley et al., 2008; this study) and estimated annual precipitation $\delta^{18}O$ (Bowen and Revenaugh, 2003; Bowen, 2022) for Maverick-Medicine HMA (tooth enamel = 23.0‰; precipitation = −13.4‰), Pilot Mountains (23.8‰, −14.5‰) and the Red Rock HMA (27.8‰, −10.5‰; data from Lachniet et al., 2020, imply a value of −10.3‰). We assign errors of ±2‰ and ±1.4‰ to the data from Crowley et al. (2008) and the Red Rock HMA, respectively. Although we could regress these data to develop a local calibration of water $\delta^{18}O$ vs. tooth enamel $\delta^{18}O$, data scatter and limited compositional range would confer large uncertainties to any inferred slope and intercept. To constrain possible values for slope (m), we note that oxygen mass balance and physiology impose a minimum value of 1.0 (Kohn, 1996; the inverse of the slope discussed in section 3.1), and that $\delta^{18}O$ values for modern equines, bovines, and elephants overlap nearly completely (Kohn and Cerling, 2002). Simultaneously regressing the global dataset for these three groups yields a best-fit slope of m = 1.12 (±0.07, 2σ). Assuming this slope, a calibration intercept is then determined from a weighted average of the data from Nevada: b ~ −40.7‰. Thus, our final expression is:

$$\delta^{18}O_{water}(‰, VSMOW) = 1.12 \cdot \delta^{18}O_{tooth\ enamel}(‰, VSMOW) - 40.7 \quad (2)$$

The uncertainty in this expression is at least 1‰, reflecting data

Table 1
Mean, maximum, and minimum $\delta^{13}C$ and $\delta^{18}O$ values for all browsers and grazers. Identification number, location, unit, taxon, tooth, error, and ages are also included.

ID Number	TUSK location	Repository	Unit	Taxon/species	Tooth	mean $\delta^{13}C$	2 s.e.	max $\delta^{13}C$	min $\delta^{13}C$	mean $\delta^{18}O$	2 s.e.	max $\delta^{18}O$	min $\delta^{18}O$	Age (cal ka BP)	±	$\delta^{13}C$ plant	$\delta^{18}O$ water	$\delta^{13}C$ atm	% C_4	±
LVWH1	N/A	BSU		*Equus caballus*	M/P	−9.79	0.69	−8.11	−12.58	31.94	1.62	36.88	27.81	0	0	−24.65	−4.9	−8.00	3	12
LVWH2	N/A	BSU		*Equus caballus*	M/P	−9.69	0.75	−8.05	−11.18	25.14	0.70	26.43	23.38	0	0	−24.55	−12.5	−8.00	3	12
LVWH3	N/A	BSU		*Equus caballus*	M/P	−9.97	0.38	−8.87	−11.58	29.40	0.64	31.58	26.93	0	0	−24.83	−7.8	−8.00	1	11
LVWH4	N/A	BSU		*Equus caballus*	M/P	−8.39	0.27	−7.35	−9.05	25.80	0.54	27.49	24.36	0	0	−23.22	−11.8	−8.00	14	10
LVWH5	N/A	BSU		*Equus caballus*	M/P	−10.83	0.88	−7.61	−13.03	28.79	0.74	30.88	26.92	0	0	−25.70	−8.5	−8.00	−5	13
LVWH6	N/A	BSU		*Equus caballus*	M/P	−9.13	0.35	−8.30	−11.45	26.81	1.13	31.99	24.03	0	0	−23.98	−10.7	−8.00	8	11
LVWH7	N/A	BSU		*Equus caballus*	M/P	−9.56	0.13	−9.11	−10.16	27.34	0.98	30.82	24.67	0	0	−24.42	−10.1	−8.00	4	11
LVWH8	N/A	BSU		*Equus caballus*	M/P	−9.11	0.74	−7.20	−11.17	25.85	0.87	27.79	22.40	0	0	−23.96	−11.7	−8.00	8	12
LVWH9	N/A	BSU		*Equus caballus*	M/P	−9.68	0.19	−8.82	−10.27	29.33	0.47	30.90	27.48	0	0	−24.54	−7.9	−8.00	4	11
A.4861	N/A	N/A	E1	*Equus*[a]	X	−7.70				24.9				14.75	1.35	−22.53	−12.8	−6.64	9	10
n/a	N/A	N/A	E1	*Equus*[a]	P	−6.30				25.1				14.75	1.35	−21.11	−12.6	−6.64	20	10
64252	N/A	N/A	E1	*Equus*[a]	X	−8.90				24.0				14.75	1.35	−23.74	−13.8	−6.64	−1	11
64525	N/A	N/A	E1	*Camelops*[a]	P	−9.60				24.8				14.75	1.35	−23.62		−6.64	0	11
64268	N/A	N/A	E1	*Camelops*[a]	M1/2	−8.00				25.8				14.75	1.35	−22.00		−6.64	13	10
A.4901	N/A	N/A	E1	*Camelops*[a]	X	−8.70				27.7				14.75	1.35	−22.71		−6.64	7	10
A.5494	N/A	N/A	E1	*Mammuthus*[a]	X	−8.90				24.9				14.75	1.35	−23.74	−12.8	−6.64	−1	11
A.4592	N/A	N/A	E1	*Mammuthus*[a]	X	−7.90				27.7				14.75	1.35	−22.73	−9.7	−6.64	7	10
n/a	N/A	N/A	E1	*Mammuthus*[a]	X	−8.90				23.2				14.75	1.35	−23.74	−14.7	−6.64	−1	11
64393	N/A	N/A	E1	*Mammuthus*[a]	M3	−8.30				20.6				14.75	1.35	−23.14	−17.6	−6.64	4	11
64393	N/A	N/A	E1	*Mammuthus*[a]	P	−9.00				20.6				14.75	1.35	−23.85	−17.6	−6.64	−1	11
L3160-1015a	00005	LVNHM	E1d	*Equus*	X	−8.70	0.23	−8.25	−9.49	32.72	0.84	34.27	29.80	13.70	0.11	−23.54	−4.0	−6.59	1	11
L3160-1015b	00005	LVNHM	E1d	*Equus*	I	−7.05	0.24	−6.63	−7.70	23.28	0.31	23.78	22.31	13.70	0.11	−21.04	−14.6	−6.59	13	10
L3160-1016	00005	LVNHM	E1d	*Equus*	dP	−9.1	0.4	−8.6	−9.5	24.86	0.96	26.10	23.77	13.70	0.11	−23.99	−12.9	−6.59	−3	11
L3160-1186	00092	LVNHM	E1b	*Mammuthus*	X	−11.63	0.12	−11.35	−11.97	18.86	0.24	19.37	18.35	14.41	0.19	−26.52	−19.6	−6.61	−22	12
L3160-1127-1131	00001	LVNHM	E1b	*Mammuthus*	X	−7.99	0.18	−7.51	−8.59	18.87	0.11	19.18	18.32	14.41	0.19	−22.82	−19.6	−6.61	6	10
03GAM10−15.1.1	00321	LVNHM	E1b	*Mammuthus*	X	−7.30	0.30	−6.74	−7.67	19.77	0.33	20.32	19.36	14.41	0.19	−22.12	−18.6	−6.61	12	10
03GAM10−15.1.2	00321	LVNHM	E1b	*Mammuthus*	X	−6.99	1.38	−5.63	−7.87	20.28	0.24	20.41	20.04	14.41	0.19	−21.80	−18.0	−6.61	14	10
03GAM10−15.1.3	00321	LVNHM	E1b	*Mammuthus*	X	−8.16	0.94	−7.41	−9.03	21.02	0.53	21.47	20.56	14.41	0.19	−22.99	−17.2	−6.61	5	10
03GAM10−15.1.4	00321	LVNHM	E1b	*Mammuthus*	X	−7.37	0.20	−6.75	−7.87	20.08	0.25	20.67	19.46	14.41	0.19	−22.20	−18.2	−6.61	11	10
L3160-1255	00053	LVNHM	E1b	*Camelops*	X	−8.21	0.37	−7.20	−9.08	23.92	0.35	24.86	22.94	14.41	0.19	−22.21		−6.61	11	10
03MRR 10-1.2	00048	LVNHM	E1a	*Equus*	X	−7.44	0.27	−6.46	−8.26	25.25	0.36	26.20	24.37	15.57	0.54	−22.27	−12.4	−6.70	11	10
10CM6-17.1	00467	LVNHM	E1a	*Camelops*	M	−9.40	0.19	−9.10	−9.79	25.99	2.10	30.19	22.99	15.36	0.21	−23.42		−6.68	2	11
10CM6-17.2	00468	LVNHM	E1a	*Camelops*	M3	−4.02	0.74	−2.69	−5.15	22.52	0.87	24.18	21.21	15.36	0.21	−17.97		−6.68	44	11
L3160-875	00205	LVNHM	E0	*Mammuthus*	X	−8.24				20.83				20.64	2.40	−23.08	−17.4	−6.46	3	11
L3088-390a	00662	NVSM	E0	*Bison*	M3	−7.71	0.06	−7.63	−7.79	21.63	0.12	21.81	21.44	20.64	2.40	−22.53	−16.5	−6.46	7	10
L3160−207.1	00287	LVNHM	E0	*Equus*	M	−5.57	0.44	−5.12	−6.17	22.99	0.52	23.61	22.34	20.64	2.40	−20.37	−15.0	−6.46	24	10
L3160−207.2	00287	LVNHM	E0	*Equus*	M	−5.63	0.56	−4.86	−6.51	22.21	0.49	22.87	21.56	20.64	2.40	−20.43	−15.8	−6.46	23	11
L3160−654.2	00172	LVNHM	E0	*Equus*	M	−3.01	0.39	−2.81	−3.20	22.63	0.04	22.65	22.61	20.64	2.40	−17.76	−15.4	−6.46	44	10
L3160−654.1	00172	LVNHM	E0	*Equus*	M	−8.80	0.19	−8.61	−8.90	32.05	1.03	32.90	31.12	20.64	2.40	−23.64	−4.8	−6.46	−1	11
L3088-520	00656	NVSM	E0	*Camelops*	I	−5.88	0.35	−4.71	−7.01	24.12	0.35	25.39	22.92	19.50	0.14	−19.86		−6.39	27	10
L3088-459	00656	NVSM	E0	*Camelops*	P4	−6.00	0.45	−4.87	−7.00	23.01	0.37	23.90	22.24	19.50	0.14	−19.98		−6.39	26	10
L3160-953	00163	LVNHM	E0	*Camelops*	M2	−10.69	0.54	−8.74	−11.63	25.71	0.28	26.28	24.72	19.50	0.14	−24.73		−6.39	−10	12
L3160−773.1	00169	LVNHM	E0	*Camelops*	I1	−7.71	0.46	−6.89	−8.98	22.02	0.42	23.69	21.16	19.50	0.14	−21.71		−6.39	13	11
L3160−773.2	00169	LVNHM	E0	*Camelops*	I2	−7.39	0.04	−7.37	−7.41	20.97	0.72	21.32	20.61	19.50	0.14	−21.39		−6.39	16	10
L3160−773.3	00169	LVNHM	E0	*Camelops*	I	−8.16	0.74	−6.59	−9.63	20.98	0.47	21.67	20.25	19.50	0.14	−22.16		−6.39	10	10
L3088-391	00662	NVSM	E0	*Camelops*	M2	−6.58	0.22	−5.77	−7.66	22.88	0.17	23.75	22.28	19.50	0.14	−20.56		−6.39	22	10
64501	N/A	N/A	D	*Mammuthus*[a]	M3	−6.40				22.80				33.00	6.00	−21.21	−15.2	−6.45	17	10
n/a	N/A	N/A	D	*Equus*[a]	X	−9.80				25.40				33.00	6.00	−24.66	−12.3	−6.45	−9	11
L3160-39a	00221	LVNHM	D2	*Mammuthus*	X	−4.73	0.27	−3.64	−6.14	20.42	0.14	21.05	19.69	29.64	2.09	−19.51	−17.8	−6.40	30	10

L3160-6	00221	LVNHM	D2	*Mammuthus*	P1	−4.36	0.18	−3.28	−5.30	20.66	0.14	21.71	19.76	29.64	2.09	−19.14	−17.6	−6.40	33	10
L3160-917	00206	LVNHM	D1	*Bison*	P/M	−2.36	0.33	−1.43	−3.06	21.87	0.58	23.48	20.79	35.54	2.48	−17.10	−16.2	−6.56	50	10
L3160-781	00206	LVNHM	D1	*Bison*	X	−2.90	0.47	−1.79	−3.66	21.01	0.38	21.92	20.26	35.54	2.48	−17.66	−17.2	−6.56	46	10
L3160-779	00210	LVNHM	D1	*Equus*	M	−6.11	0.37	−5.56	−6.62	22.84	0.30	23.24	22.20	35.54	2.48	−20.91	−15.1	−6.56	21	10
L3160-647	00194	LVNHM	D1	*Mammuthus columbi*	M3	−9.01	0.16	−8.59	−9.44	19.13	0.18	19.60	18.58	35.54	2.48	−23.86	−19.3	−6.56	−2	11
64692	N/A	N/A	B2	*Bison*[a]	P	−4.90				20.30				50	5	−19.69	−18.0	−6.42	29	10
64692	N/A	N/A	B2	*Bison*[a]	P2	−3.40				25.00				50	5	−18.16	−12.7	−6.42	41	10
n/a	N/A	N/A	B2	*Mammuthus*[a]	M	−6.40				19.30				50	5	−21.21	−19.1	−6.42	17	10
64250	N/A	N/A	B2	*Equus*[a]	M3	−1.60				22.50				50	5	−16.34	−15.5	−6.42	55	10
L3160-751	00136	LVNHM	B2	*Bison*	M2	−7.74	0.40	−6.96	−8.59	20.46	1.08	22.46	17.59	50	5	−22.57	−17.8	−6.42	7	11
L3160-946	00136	LVNHM	B2	*Bison*	X	−5.02	0.32	−4.53	−5.67	19.26	0.45	20.11	18.73	50	5	−19.80	−19.1	−6.42	28	10
L3160−230.4	00232	LVNHM	B2	*Bison*	M	−4.89	0.17	−4.32	−5.37	20.74	0.13	21.20	20.50	50	5	−19.68	−17.5	−6.42	29	10
L3160−818.2	00135	LVNHM	B2	*Bison*	M	−3.74	0.35	−3.28	−4.26	20.94	0.58	21.61	20.03	50	5	−18.51	−17.3	−6.42	38	10
L3160-748	00137	LVNHM	B2	*Equus*	X	−4.05	0.26	−3.49	−4.41	20.26	0.75	21.30	18.39	50	5	−18.83	−18.0	−6.42	35	10
L3160−230.2	00232	LVNHM	B2	*Equus*	M	−4.84	0.15	−4.07	−5.56	20.91	0.11	21.35	20.57	50	5	−19.62	−17.3	−6.42	29	10
04MRR1-28.1	00258	LVNHM	B1	*Bison*	M	−2.64	0.39	−2.14	−3.46	24.10	0.85	25.42	22.82	72	8	−17.39	−13.71	−6.42	47	10

BSU = Boise State University; LVNHM = Las Vegas Natural History Museum; NVSM = Nevada State Museum. P = premolar, M = molar, I = incisor, X = fragment.
[a] Data from Connin et al. (1998) from the Las Vegas area (but without information about zoning or variability).

scatter for equids. We caution that this calibration has no validity outside the interior western U.S., and possibly not outside Nevada. Simpler predictive approaches, for example subtracting tooth enamel isotope compositions of Pleistocene taxa vs. modern equids and scaling by a factor of 1.0–1.2, do not yield substantially different conclusions.

5.5. Estimated C_4 grass abundance

We estimated the fraction of C_4 vegetation consumed by different herbivores using $\delta^{13}C$ values from tooth enamel in reference to atmospheric $\delta^{13}C$ values and modern (2000 AD) isotopic compositions of C_3 and C_4 plants. Vegetation $\delta^{13}C$ values for the age of the fossil were first calculated using Eq. (1), assuming ε^* of 14.5‰ for *Equus*, *Bison* and *Mammuthus* and 13.7‰ for *Camelops* (Passey et al., 2005). Isotopic discrimination for that time (ε^*_t) between vegetation ($\delta^{13}C_{diet}$) and the $\delta^{13}C$ of atmospheric CO_2 ($\delta^{13}C_{atm}$) was then calculated:

$$\varepsilon^*_t = \frac{\delta^{13}C_{atm} - \delta^{13}C_{diet}}{1 + \delta^{13}C_{diet/1000}} \quad (3)$$

That same ε^*_t discrimination was then applied to a 2000 AD atmospheric $\delta^{13}C$ value of −8.0‰ to determine the equivalent isotopic composition of modern vegetation ($\delta^{13}C_{diet,\ modern}$). The percent C_4 vegetation in herbivore diets was then estimated using the following expression:

$$\%_{C_4} = 100\% \cdot \frac{(\delta^{13}C_{diet,modern} - \delta^{13}C_{C_3})}{(\delta^{13}C_{C_4} - \delta^{13}C_{C_3})} \quad (4)$$

where carbon isotope compositions of C_3 and C_4 vegetation reflect modern compilations: $\delta^{13}C$ ~ −25 ± 1‰ for C_3 vegetation in dry ecosystems (Kohn, 2010) and −12 ± 1‰ for C_4 vegetation (Cerling et al., 1997).

Uncertainties in percent C_4 are approximately ±10–12%. These represent the propagated 2 s.e. variability in tooth enamel compositions (which ranges between ~±0.2 and ± 1.4‰ for this study, but is unknown for data of Connin et al., 1998), ±1‰ in typical compositions of C_3 and C_4 plants, and ±1‰ uncertainty in isotopic discrimination between tooth enamel and diet $\delta^{13}C$. Each error was propagated separately then combined quadratically.

6. Results

6.1. Oxygen and carbon isotopes in tooth enamel

Nearly all teeth have broadly compatible compositions within a member or bed, permitting close statistical comparisons. However, outliers in $\delta^{18}O$ occur for specimens 03KS9-23.1 (bed E_{1d}; 32.7‰; *Equus*) and L3160−654.1 (bed E_0; 32.0‰; *Equus*). We omit these two teeth from calculations and interpretations. Mean grazer tooth enamel $\delta^{18}O$ values from beds E_0 and E_1 are +22.1 ± 0.8‰ (2 s.e.) and +22.5 ± 1.3‰, respectively, slightly higher than grazer tooth enamel from members B (+21.2 ± 1.1‰) and D (+21.8 ± 1.4‰; Fig. 3; Tables 1 and 2; p = 0.01). These values are all 5–6‰ lower than the modern equid average or median (~27.8 ± 1.5‰). *Camelops* tooth enamel $\delta^{18}O$ values from beds E_0 and E_1 are +22.8 ± 1.3‰ and +25.1 ± 1.5‰, respectively, which are ~2‰ higher than for sympatric grazers (Fig. 4; Tables 1 and 2), although the difference is not statistically significant.

Mean tooth enamel $\delta^{13}C$ values from grazers from beds E_0 and E_1 are −6.5 ± 1.8‰ and −8.2 ± 0.6‰, respectively, and are significantly lower than mean grazer $\delta^{13}C$ values from members B (−4.5 ± 1.0‰)

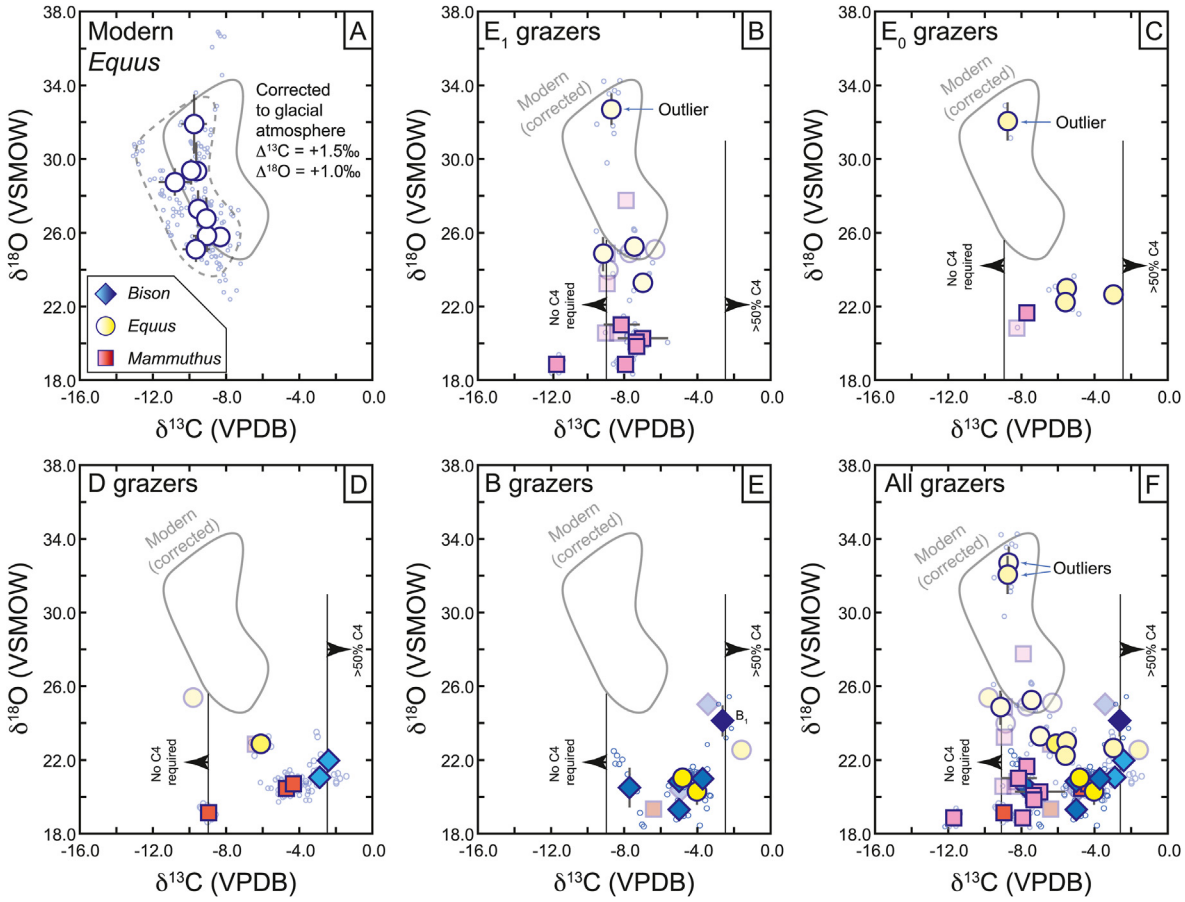

Fig. 3. Tooth enamel $\delta^{13}C$ and $\delta^{18}O$ values for grazers (*Bison* = diamonds, *Mammuthus* = squares, and *Equus* = circles; key in panel A). Large symbols are average compositions for each tooth with 2 s.e. bars. Small circles are individual measurements. (A) Modern data; boundary is drawn by eye and has no statistical significance. Solid boundary accounts for secular changes to carbon isotope compositions of atmospheric CO_2 and oxygen isotope composition of seawater and the global meteoric cycle. This boundary is repeated in other panels for fossil data to facilitate comparisons. (B) Bed E_1, (C) Bed E_o, (D) Member D, (E) Member B, and (F) all fossil data. Lower $\delta^{18}O$ values for fossils compared to modern suggest an increase in proportion of high-latitude, winter moisture (supporting the SOW hypothesis). Higher $\delta^{13}C$ values for fossils compared to modern suggest an increase in proportion of low-latitude, summer moisture (apparently supporting the OOT hypothesis).

and D (−5.7 ± 1.9‰; Tables 1 and 2). These values are all much higher than for modern equids (−9.6 ± 0.4‰; Fig. 3; Table 2). *Camelops* from beds E_0 and E_1 has mean $\delta^{13}C$ values of −7.5 ± 1.2‰ and −8.0 ± 1.7‰, respectively, indistinguishable from grazers.

6.2. Isotope zoning in teeth

With a few rare exceptions (e.g., *Equus* L3160–230.2, L3088-390a), all modern and fossil teeth show resolvable isotopic zoning (Fig. 5). In many teeth, $\delta^{13}C$ trends in opposition to $\delta^{18}O$ (e.g., Fig. 5A, C, J, M, N), but other teeth show parallel trends (e.g., Fig. 5B, G). Some teeth show both parallel and opposite trends in different parts of the tooth (e.g., Fig. 5E).

6.3. Inferred oxygen isotope compositions of local water

Eq. (2) as applied to *Equus*, *Bison* and *Mammuthus* implies statistically different ($p = 0.007$) mean $\delta^{18}O_{water}$ values of ~ −15.6‰ for Bed E and −16.6‰ for combined beds B and D (Fig. 6; Table 1).

6.4. %C_4 in grazer diet

Modern *Equus* compositions imply horses in Nevada consume essentially no C_4 grass on average (4 ± 4%, 2 s.e.; range = −5 to 14%; Fig. 7; Table 1), even though C_4 grasses are widespread in the area where these animals lived. The maximum C_4 plant consumption recorded in several teeth, based on maximum $\delta^{13}C$, approaches 15%, and in two teeth are 20–25%. Grazer tooth enamel compositions from beds E_0 and E_1 (~23–13 ka), suggest C_4 grass consumption of 8 ± 5% (range = 0–44%; Fig. 7; Table 1). Grazer tooth enamel from older members B and D (~78–29 ka) imply higher C_4 grass consumption of 28 ± 8% (2 s.e.; range = 0–55%; Fig. 7; Table 1). These temporal differences in C_4 consumption are significant ($p = 4 \times 10^{-5}$; Table 2). *Camelops* compositions for beds E_0 and E_1 imply consumption of 14 ± 8% C_4 vegetation (range = 0–44%; Fig. 7; Table 1).

7. Discussion

7.1. Compositional comparisons among taxa and times

Carbon and oxygen compositions of the sympatric grazers *Equus*, *Bison* and *Mammuthus* largely overlap (Fig. 3). This implies similar dietary selection and water dependence among these taxa, like their modern representatives (horse, bison) and nearest relatives (elephants) who are all grazers and water-dependent. Analysis of these same Pleistocene taxa in other areas of western North America (but without a highly resolved chronology) also shows substantial compositional overlap, although different species of *Equus* can show significantly different $\delta^{13}C$ values, and *Mammuthus*

Table 2
Statistical comparisons of isotope data from modern and late Pleistocene tooth enamel from the Las Vegas area. Bold values are significant.

Group	Modern All Pleistocene grazers	E grazer	E_1 grazer	E_0 grazer	D grazer	B grazer	B&D grazer	*Camelops* vs. grazer $\delta^{13}C$	E_1 *Camelops*	E_0 *Camelops*	E *Mammuthus*	E *Equus*	B&D *Mammuthus*	B&D *Equus*	B&D *Bison*	Bed E inferred water	Beds B&D inferred water	Modern *Equus* % C_4	Mean grazer %C_4	Bed E grazer %C_4	Beds B&D grazer % C_4	Camel %C_4
Mean $\delta^{13}C$	−9.57	−7.78	−8.20	−6.49	−5.71	−4.47	−4.99	−7.72	−7.99	−7.49	−8.39	−7.11	−6.18	−5.28	−4.18			4	17	8	28	14
2 s.e.	0.45	0.66	0.56	1.77	1.89	1.02	1.00	0.99	1.67	1.25	0.70	1.13	1.65	2.70	1.12			4	5	5	8	8
Mean $\delta^{18}O$	27.82	22.43	22.54	22.06	21.77	21.25	21.47	23.88	25.12	22.81	21.39	24.73	20.46	22.38	21.56	−15.62	−16.65					
2 s.e.	1.47	0.68	1.02	1.31	0.76	1.36	1.12	0.85	1.14	1.47	1.29	1.51	1.77	1.31	1.79	1.24	1.19	0.95				

t-tests	Modern *Equus* +1.5‰ vs. E grazers $\delta^{13}C$	**Modern *Equus* + 1.5‰ vs. B&D grazers $\delta^{13}C$**	**E vs. B&D grazer $\delta^{13}C$**	**E vs. B&D&Grazer %C_4**	*Camelops* vs. grazer $\delta^{13}C$	*Equus* vs. Mammuthus $\delta^{13}C$	B&D *Bison* vs. *Equus* & *Mammuthus* $\delta^{13}C$	**E vs. B&D *Mammuthus* $\delta^{13}C$**	**E vs. B&D *Equus* $\delta^{13}C$**	**E vs. B&D&Grazer $\delta^{18}O$**	*Camelops* vs. grazer $\delta^{18}O$	*Equus* vs. *Mammuthus* $\delta^{18}O$	B&D *Bison* vs. *Equus* & *Mammuthus* $\delta^{18}O$	E vs. B&D *Mammuthus* $\delta^{18}O$	**E vs. B&D *Equus* $\delta^{18}O$**
	0.51	**9.3E-06**	**3.6E-05**	**1.6E-04**	0.90	0.48	0.51	**4.5E-03**	**2.8E-04**	**1.1E-02**	0.76	0.66	0.90	0.25	**6.8E-03**

$\delta^{18}O$ values range from overlapping to ~2‰ lower than *Equus* and *Bison* (Connin et al., 1998; Kohn and McKay, 2012; Pérez-Crespo et al., 2012a, b; Trayler et al., 2015; Bravo-Cuevas et al., 2017). Although modern compositional overlap supports our regression of modern equid, bovine, and elephant $\delta^{18}O$ values to determine the slope of Eq. (2), calculated water compositions based on *Mammuthus* $\delta^{18}O$ may be ~1‰ too low. Such a bias does not affect our interpretations of moisture sources and seasonality significantly.

Relatively high $\delta^{13}C$ values for late Pleistocene *Camelops* (Fig. 4) indicate moderate (14 ± 8%, 2 s.e., but in one case >40%) consumption of C_4 plants. Because *Camelops* was a browser (Semprebon and Rivals, 2010; Yann et al., 2016), and modern camels preferentially consume *Atriplex* (Towhidi et al., 2011), which in the western U.S. is C_4 (Kadereit et al., 2010), the relatively high $\delta^{13}C$ values for *Camelops* almost certainly indicate C_4 *Atriplex* consumption during the late Pleistocene (Vetter, 2007). Today, *Atriplex* constitutes over 15% of land cover in the Las Vegas Valley (Shanahan et al., 2007). Although we cannot determine whether *Atriplex* had higher or lower abundance during the late Pleistocene, its persistence is consistent with warm, dry summers. These conditions generally support the SOW hypothesis (very wet winters, dry summers) more than the OOT hypothesis (moderately wet winters and wet summers). Mean $\delta^{18}O$ values for *Camelops* are generally but not statistically higher than for sympatric grazers (23.8 ± 1.1 vs. 22.4 ± 1.0‰; Tables 1 and 2). This might suggest greater drought-tolerance for *Camelops*, but more data are required to confirm a systematic offset.

7.2. Oxygen isotopes and inferred water compositions support the SOW model

Relative to modern $\delta^{18}O_{water}$ values from the Las Vegas Valley (−10.5‰; Bowen and Revenaugh, 2003; Lachniet et al., 2020; Bowen, 2022), fossil tooth enamel compositions suggest that $\delta^{18}O_{water}$ values (~-16‰) in the late Pleistocene were lower by about 5–6‰ (Fig. 6; Table 2). Even modern spring water in the Great Basin, which is heavily biased to seasonal winter precipitation (Lachniet et al., 2020), has higher $\delta^{18}O_{water}$ values (−12.9‰, or ~3‰ higher than in the Pleistocene; Friedman, 2000). This difference between modern and Pleistocene $\delta^{18}O_{water}$ values is broadly compatible but much more pronounced than regional compilations of $\delta^{18}O_{water}$ values for the late Pleistocene (~2‰ lower; Jasechko et al., 2015; Jasechko, 2016), although our temporal data are more highly resolved than other datasets. Secular changes in global $\delta^{18}O_{water}$ do not mitigate this difference, rather correcting for ice volume (~1‰ effect) would increase the difference to 6–7‰ (annual precipitation), albeit ~4‰ relative to modern winter precipitation. Pleistocene speleothem $\delta^{18}O$ values for Leviathan Cave in south-central Nevada are 4–5‰ lower than Holocene values (Lachniet et al., 2014, 2017, 2020). If Pleistocene temperature was lower (as seems likely) water $\delta^{18}O$ values must have been at least 4–5‰ lower at this location, commensurate with our interpretations. Both results suggest systematic errors in isotope-enabled GCMs such that precipitation $\delta^{18}O_{water}$ is overestimated in the southwestern US during the latest Pleistocene.

The lower $\delta^{18}O_{water}$ values during the late Pleistocene compared to today (Fig. 6; Table 2) are consistent with an increase in winter precipitation or a decrease in temperature (or both; Fig. 1A; Lachniet et al., 2014, 2017, 2020). These observations strongly support the SOW hypothesis, in which increased winter precipitation was sourced from higher latitudes and fell across a generally colder landscape (Lachniet et al., 2014, 2017, 2020). An increase in winter precipitation logically recharged groundwater more than it does today, leading to enhanced discharge of low-$\delta^{18}O$ water on valley floors.

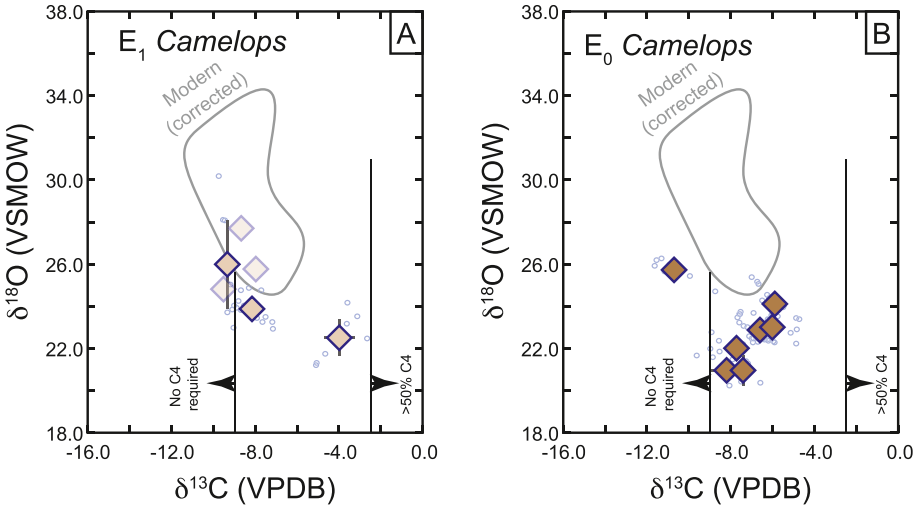

Fig. 4. Tooth enamel $\delta^{13}C$ and $\delta^{18}O$ values for *Camelops* (A) Bed E_1, (B) Bed E_o. Some *Camelops* have relatively high $\delta^{13}C$ values, suggesting the consumption of *Atriplex*, a C_4 shrub that thrives in environments with low amounts of summer precipitation. The solid boundary is the same as in Fig. 3 and is based on modern *Equus* compositions.

7.3. Carbon isotopes and $\%C_4$ in grazers appear to support the OOT model

Pleistocene grazers (including equids) consumed considerably more C_4 grass than modern equids, especially during deposition of members B and D when $\%C_4$ consumption ranged up to 50% (Fig. 7; Table 2). Conventionally, higher calculated $\%C_4$ consumption by late Pleistocene grazers has been assumed to reflect higher environmental $C_4/(C_4 + C_3)$ and either increased summer precipitation or decreased CO_2 concentrations (or both; e.g., Connin et al., 1998; Koch et al., 2004; Cotton et al., 2016; Fig. 1B). Thus, in comparison with modern equid compositions, higher $\%C_4$ consumption by late Pleistocene grazers *appears* to support the OOT hypothesis better than the SOW hypothesis. Support for the OOT hypothesis contradicts the interpretations derived from oxygen isotope data presented in section 7.2.

7.4. Reconciling climatic interpretations of oxygen and carbon isotope data

Hypothetically, the different interpretations derived from $\delta^{18}O$ vs. $\delta^{13}C$ (and $\%C_4$) data might be reconciled if summer precipitation increased C_4 abundances, but herbivores derived most of their water from winter-sourced springs and wetlands. Colder winters might lower $\delta^{18}O$ of local water and teeth of the herbivores that drank it, while higher $C_4/(C_4 + C_3)$ raised grazer $\delta^{13}C$. This scenario could support both the SOW and OOT models. A similar interpretation was advanced to explain isotope and floral data in New Mexico (Asmerom et al., 2010) and is implicit in the models of Connin et al. (1998). However, isotope zoning in teeth (Fig. 5G-O) does not strongly resemble zoning in latest Pleistocene mammoth teeth from southeastern Arizona (Fig. 5F; Metcalfe et al., 2011), which is subject to much more abundant seasonal summer precipitation than southern Nevada. The OOT model also seems unlikely in the context of isotopic mass balance in animals. In general, even water-dependent animals derive most of their oxygen from food sources, rather than drinking water (Kohn, 1996). If summer precipitation increased C_4 grass abundances, grazers should show $\delta^{18}O$ values characteristic of summer precipitation at least sometime during the year. Yet, isotope zoning along teeth does not show $\delta^{18}O$ values that exceed modern averages except for teeth that have low $\delta^{13}C$, which is inconsistent with summer food consumption (e.g., outliers L3160-1015a and L3160-654 with $\delta^{18}O > 30‰$, but $\delta^{13}C < -8‰$). In fact, more typical maximum $\delta^{18}O$ values of ~25‰, corrected downwards by 1‰ for ice volume, would correspond with typical minimum values measured in equids in the region today. The lack of evidence for summer precipitation in numerous seasonally resolved data makes the OOT model seem unlikely.

How, then, can we explain the higher $\%C_4$ in Pleistocene grazers? We hypothesize that dietary competition in the context of a more diverse and abundant Pleistocene fauna drove grazers to feed preferentially on C_4 grasses, even though $C_4/(C_4 + C_3)$ was actually lower than today. The rationale for this interpretation is as follows.

First, isotopic compositions of modern equids in the Las Vegas area do not reflect modern $C_4/(C_4 + C_3)$. Grasses today constitute a small fraction of total plant biomass in Nevada deserts, typically <5% (e.g., see summary of Paruelo and Lauenroth, 1996) but locally grassy regions do occur (Webb et al., 2003; Shanahan et al., 2007). Of modern grasses, 55–60% of species regionally are C_4 (https://www.nps.gov/im/mojn/inventories.htm, accessed 2018 for Death Valley National Park, Mojave National Preserve, and Lake Mead National Recreation Area), while nearly 75% of the grasses in the Las Vegas area are C_4 (Shanahan et al., 2007). High $C_4/(C_4 + C_3)$ reflects a modern warm-dry climate that receives about subequal amounts of winter and summer precipitation (https://wrcc.dri.edu, accessed 2021). If species abundances correspond even roughly with plant biomass, low $\delta^{13}C$ values and calculated $\%C_4$ for wild horse in the region do not represent modern grass ecology. Rather, these equids must preferentially consume C_3 plants – either C_3 grasses, or herbs, trees, and shrubs. In the western U.S., grasses typically constitute 80–90% of horse diet (Scasta et al., 2016). Thus, it would appear that, given the opportunity, equids preferentially consume C_3 grass. Without other considerations, this conclusion might indicate an even higher $C_4/(C_4 + C_3)$ grass during the Pleistocene than we calculated from grazer $\delta^{13}C$.

However, large mammal diversity during the late Pleistocene was considerably higher than today, and included numerous browsing species, such as sloths and deer, as well as camelid and antilocaprid mixed feeders (Scott et al., 2017). Niche partitioning among Pleistocene faunas is well-documented isotopically elsewhere in North America (e.g., MacFadden and Cerling, 1996; Kohn et al., 1998; Feranec and MacFadden, 2000; Kohn et al., 2005; Hoppe and Koch, 2006; DeSantis et al., 2009; Kohn and McKay, 2012; Pérez-Crespo et al., 2012a; Trayler et al., 2015; Yann et al.,

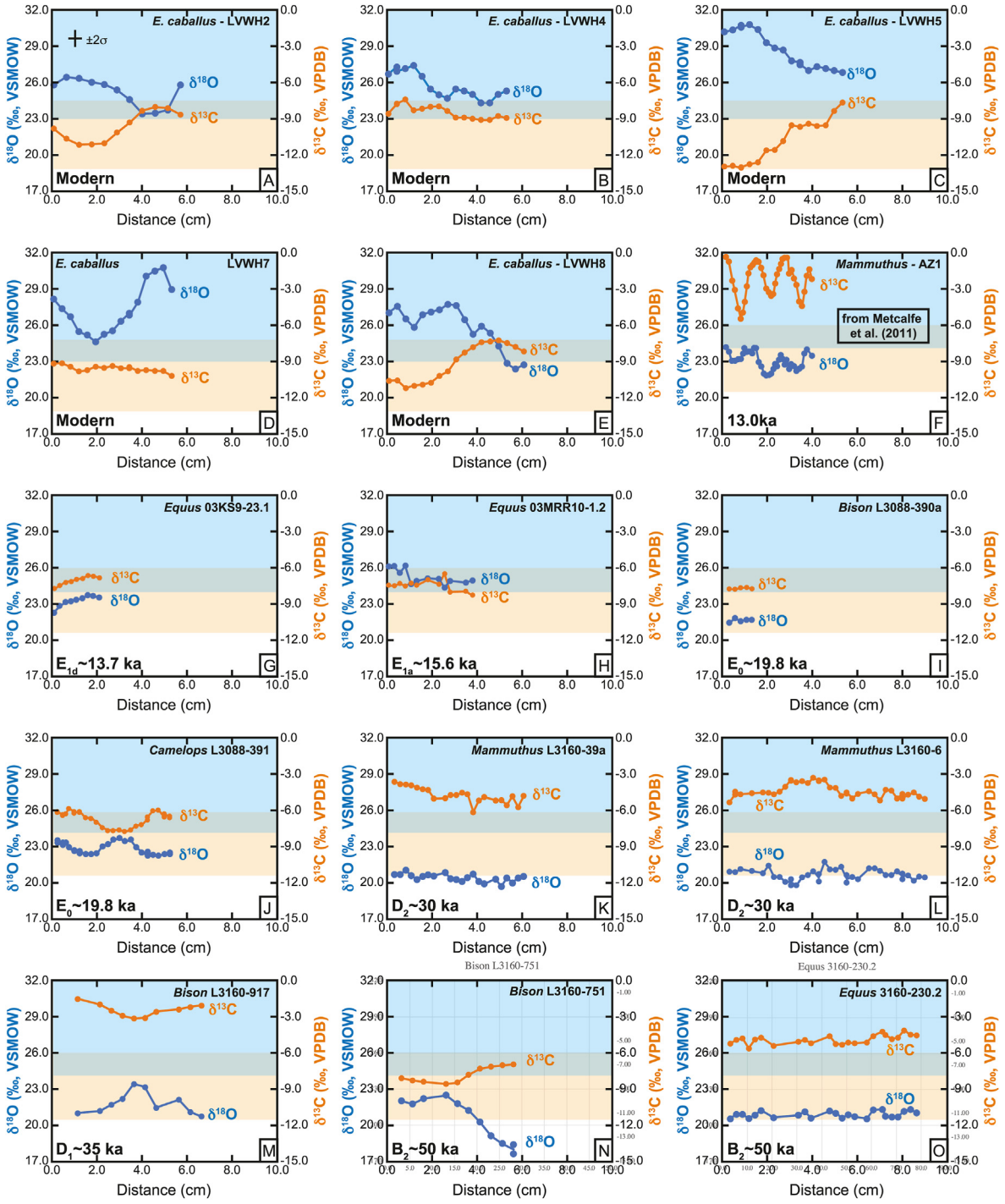

Fig. 5. Tooth enamel $\delta^{13}C$ and $\delta^{18}O$ zoning. Orange and blue fields show typical ranges of $\delta^{13}C$ and $\delta^{18}O$ values for modern *Equus* teeth and omit a few isotopically extreme values (e.g., low $\delta^{18}O$ values for LVWH8). For fossil teeth, these regions are superimposed for comparison, but adjusted for secular changes to $\delta^{13}C$ and $\delta^{18}O$ values. In general, $\delta^{13}C$ values in fossils fall above or towards the upper limit of the orange field of modern teeth, while $\delta^{18}O$ values fall below or towards the lower limit of the blue field. Zoning shows both positive and negative correlations between $\delta^{13}C$ and $\delta^{18}O$ values for both modern and fossil teeth. (A–E) Modern horse (*Equus caballus*). (F) ~13 ka *Mammuthus* from southeastern Arizona (Metcalfe et al., 2011), showing strong seasonal signal in diet and water compositions. (G–J) *Equus*, *Bison*, and *Camelops* from member E, showing both correlated and anticorrelated zoning patterns. (K–M) *Mammuthus* and *Bison* from member D. (N–O) *Bison* and *Equus* from member B. Error bar in A represent analytical error. (For interpretation of the references to color in this figure legend, the reader is referred to the Web version of this article.)

2016; Bravo-Cuevas et al., 2017; Pardi and DeSantis, 2021). Following the end-Pleistocene megafaunal extinction, some surviving species shifted their diets to occupy newly vacated niches. For example, *Odocoileus* (white-tailed deer) in the southeastern U.S. shifted to low-$\delta^{13}C$ deeper forest habitats that were formerly occupied by *Tapirus* (tapir) and *Palaeolama* (a small camelid; Kohn et al., 1998; Kohn et al., 2005). It is plausible that a modern landscape that is depauperate in large herbivores could allow modern equids in Nevada to consume their preferred vegetation, which apparently does not include C_4 grass. It follows that greater

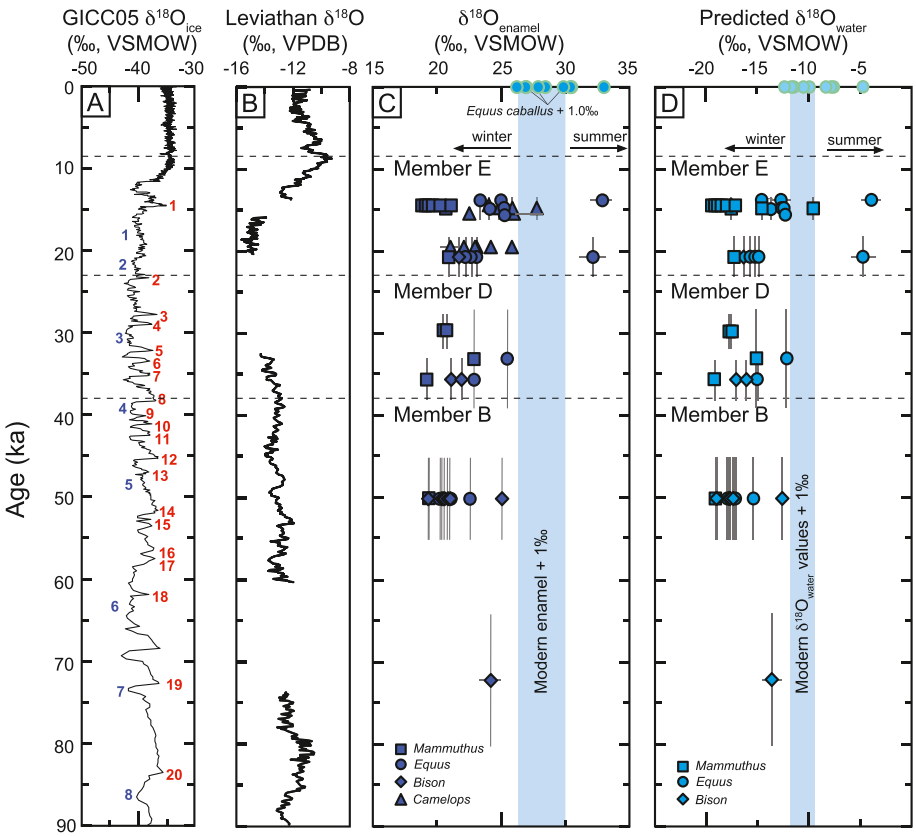

Fig. 6. Oxygen isotope data through time. Horizontal dashed lines show temporal boundaries between beds from Las Vegas Formation (Springer et al., 2015, 2018). (A) Greenland ice core reference $\delta^{18}O$ profile (GICC05; Grootes and Stuiver, 1997; Andersen et al., 2006). Blue numbers to the left of the profile refer to cold Heinrich events; red numbers to the right of the profile refer to warm Dansgaard-Oeschger events. (B) Leviathan Cave reference $\delta^{18}O$ profile (Lachniet et al., 2014, 2017, 2020). (C) Mean ± 2 s.e. $\delta^{18}O$ values of teeth. *Mammuthus* = squares, *Equus* = circles, *Bison* = diamonds, *Camelops* = triangles. Blue band represents mean ± 2 s.e. for modern *Equus* data, which adjusted upward by 1‰ to correct for isotopic effects of ice volume and facilitate comparison with data from fossils. (D) Inferred water $\delta^{18}O$ values from *Bison*, *Mammuthus*, and *Equus* fossil teeth. The blue band represents modern measured water compositions (Friedman, 2000; Bowen and Revenaugh, 2003; Lachniet et al., 2020; Bowen, 2022), adjusted upward by 1‰ to correct for isotopic effects of ice volume. Fossil teeth generally indicate lower $\delta^{18}O$ for the late Pleistocene than today, but no secular trend during the late Pleistocene is resolvable. (For interpretation of the references to color in this figure legend, the reader is referred to the Web version of this article.)

herbivore abundance overall during the late Pleistocene also increased feeding competition and more niche partitioning for the now extinct herbivores that were included in this study.

Two major implications derive from the hypothesis that greater competition among Pleistocene faunas drove grazing species to consume more C_4 grass than they would otherwise prefer. First, grazer $\delta^{13}C$ values would not necessarily reflect biomass abundances of C_3 and C_4 grasses. Besides the fact that grazers commonly consume some browse, which is nearly all C_3, competition with other species might cause grazers to increasingly consume C_4 grass, leading to apparently higher $C_4/(C_4 + C_3)$ than was actually present. In that context, existing tooth enamel-based interpretations of $C_4/(C_4 + C_3)$ should be reevaluated, including increased $C_4/(C_4 + C_3)$ in some areas during the late Pleistocene (e.g., Connin et al., 1998; Koch et al., 2004) and gradual increases in $C_4/(C_4 + C_3)$ through time (Cerling et al., 1997). Alternate isotopic archives such as paleosol carbonate or soil organic matter might provide a less biased record, although these also can have significant biases (e.g., Wynn and Bird, 2007; Sarangi et al., 2021).

Second, "high" $\%C_4$ consumption among Pleistocene grazers may actually be consistent with the SOW hypothesis. Even the maximum $\%C_4$ values calculated in this study (Fig. 7; Table 1) fall below modern $C_4/(C_4 + C_3)$ species counts. If our calculated $\%C_4$ values for Pleistocene grazers either represent $C_4/(C_4 + C_3)$ or overrepresent $C_4/(C_4 + C_3)$ because of competition with browsers and mixed-feeders, Pleistocene $C_4/(C_4 + C_3)$ may have been lower than today. Because C_4 grass abundance depends strongly on summer precipitation (Paruelo and Lauenroth, 1996), lower $C_4/(C_4 + C_3)$ during the late Pleistocene than observed today would not support the OOT hypothesis. As discussed in section 7.5, other factors, especially p_{CO2}, also influence C_4 grass abundance and further argue against an increase in summer precipitation as the driving mechanism behind the relatively high $\delta^{13}C$ values in the Pleistocene grazers analyzed in this study (Street-Perrott et al., 1997; Peng et al., 1998; Koch et al., 2004; Cotton et al., 2016).

7.5. Comparison to other studies in the southwestern U.S

Some GCMs and paleoclimate proxy studies have attributed increased late Pleistocene precipitation in the Great Basin and southwestern U.S. to increased winter precipitation in the context of the SOW model (COHMAP Members, 1988; Toggweiler et al., 2006; Wagner et al., 2010). This interpretation is generally consistent with lower $\delta^{18}O$ values in groundwater regionally (Jasechko, 2016). However, other studies have inferred increased summer (OOT) precipitation. For example, Connin et al. (1998) reported high $\delta^{13}C$ values from *Mammuthus*, *Bison*, *Equus*, and *Camelops* tooth enamel from the late Pleistocene of the southwestern U.S. and inferred high $\%C_4$, especially in southern New Mexico and Arizona. Evidence for high proportions of C_4 grasses in these areas also include plant macrofossil records from packrat middens (Holmgren et al., 2007) and stable isotope records from paleosol carbonate

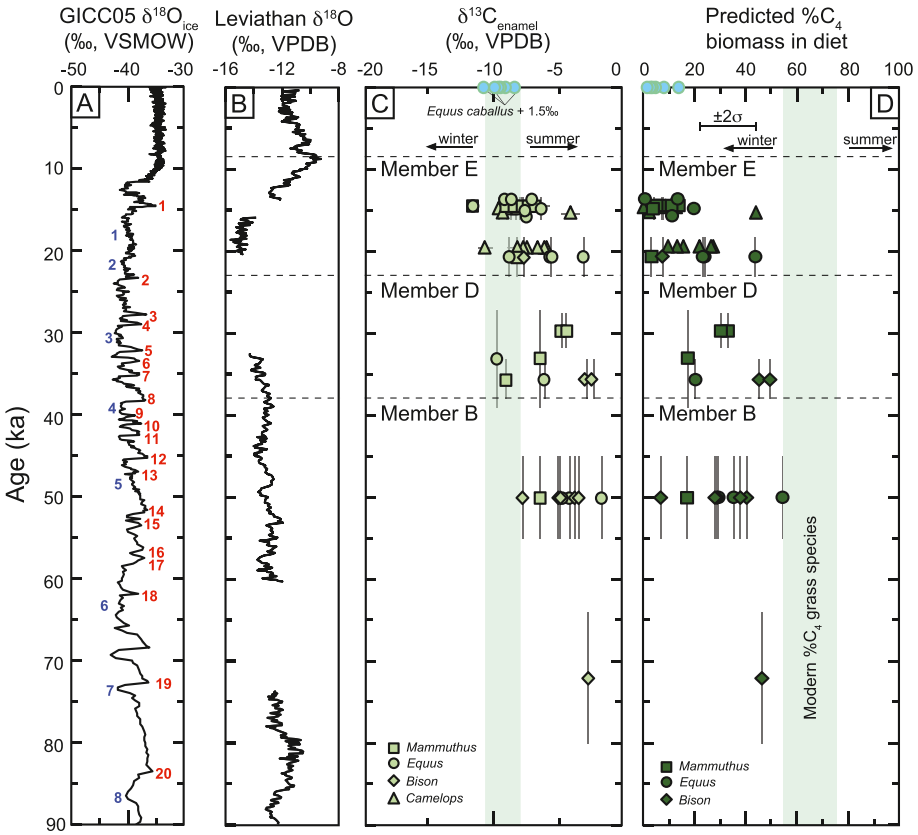

Fig. 7. Carbon isotope data through time. (A) Greenland ice core reference $\delta^{18}O$ profile (GICC05; Grootes and Stuiver, 1997; Andersen et al., 2006). Blue numbers to the left of the profile refer to cold Heinrich events; red numbers to the right of the profile refer to warm Dansgaard-Oeschger events. (B) Leviathan Cave reference $\delta^{18}O$ profile (Lachniet et al., 2014, 2017, 2020). (C) Mean ± 2 s.e. $\delta^{13}C$ values of teeth. *Mammuthus* = squares, *Equus* = circles, *Bison* = diamonds, *Camelops* = triangles. Modern data for *Equus* are bounded by green band and adjusted upward by 1.5‰ to correct for secular changes to the $\delta^{13}C$ value of atmospheric CO_2. Most data fall above modern values, indicating late Pleistocene herbivores consumed a greater proportion of C_4 plants than modern *Equus*. High $\delta^{13}C$ values for grazers and *Camelops* likely reflect consumption of C_4 grasses or the C_4 shrub *Atriplex* (saltbush), respectively. (D) Calculated percent consumption of C_4 in the grazer diet. Although most grazers consumed more C_4 grass than modern *Equus*, the calculated $\%C_4$ still falls well below observed fraction of C_4 grass species in the region today (green band). Horizontal error bar applies to all data. (For interpretation of the references to color in this figure legend, the reader is referred to the Web version of this article.)

(Monger et al., 1998). High $\delta^{13}C$ values and increased proportions of summer-flowering annuals and C_4 grasses were interpreted to reflect enhanced summer precipitation.

How can we reconcile these disparate observations derived from $\delta^{18}O$ (enhanced winter precipitation) and $\delta^{13}C$ (enhanced summer precipitation)? Asmerom et al. (2010) proposed that hydrologic systems and vegetation may be decoupled. Enhanced winter precipitation (SOW) recharged aquifers and increased spring discharge with low $\delta^{18}O$ water, while enhanced summer precipitation (either OOT or from monsoonal circulation) increased $\%C_4$ but did not cause recharge, so is not represented in either speleothem or groundwater $\delta^{18}O$ values. Similarly, in the context of $\%C_4$ predictive models, Connin et al. (1998) proposed that coupled increases in both winter and summer precipitation could explain paleoclimate proxy records in southern New Mexico and Arizona, if the proportion of summer/total precipitation during the late Pleistocene also increased to ~50–65% (vs. 40–50% today).

Two problems accompany these interpretations. First, as discussed above, $\delta^{18}O$ values for grazers (*Mammuthus*, *Bison*, and *Equus*) are never very high, even for seasonally resolved measurements. The absence of a high $\delta^{18}O$ summer signal suggests an absence of a tropical moisture source, at least in the Las Vegas Valley and possibly elsewhere in the southwestern U.S. Second, increases in summer precipitation may not be needed to explain high proportions of C_4 grasses or the $\delta^{13}C$ record of diet. Two key factors have not been previously addressed – grazer diet is approximately independent of shrub and herb abundance, and decreased p_{CO2} stabilizes C_4 grasses relative to C_3 grasses (Collatz et al., 1998). Here we reevaluate two different regional records – fossil tooth enamel (Connin et al., 1998) and combined vegetation and paleosol carbonate (Monger et al., 1998; Holmgren et al., 2007). We focus on data from southernmost Arizona and New Mexico because these areas appear to contain strong evidence for C_4 grasslands during the latest Pleistocene that has been interpreted as reflecting enhanced summer precipitation.

7.5.1. *Evaluating tooth enamel $\delta^{13}C$ records in the context of dietary partitioning*

Connin et al. (1998) report calculated $\%C_4$ of 70–80% for late Pleistocene grazers in southeastern Arizona and southwestern New Mexico. However, accounting for more recent estimates of the isotopic fractionation between tooth enamel and diet, the $\delta^{13}C$ of atmospheric CO_2 during the late Pleistocene, and more typical $\delta^{13}C$ values of C_3 plants indicates a median $\%C_4$ of ~50%. Nonetheless, some teeth from this region do indicate $\%C_4$ ~70–80%, including seasonally resolved zoning in mammoth teeth (Metcalfe et al., 2011), so it is worth considering conditions under which higher proportions of C_4 might occur. Two approaches have been used to estimate $C_4/(C_4+C_3)$. Cotton et al. (2016) correlate $\delta^{13}C$ of bison and mammoth to climate variable output of a standard GCM, but cannot independently vary climate parameters, such as input of summer moisture from the tropics. Because we wish to evaluate whether C_4/

(C_4+C_3) demands enhanced summer precipitation, we instead chose to follow Connin et al. (1998) in using equations from Paruelo and Lauenroth (1996). These equations predict abundances of C_3 grasses, C_4 grasses, and C_3 shrubs based on correlation with modern climate parameters. This latter approach readily allows assessment of how a change in a single climate parameter, such as summer precipitation, affects abundances of these different plant types.

As referenced to modern climate in Benson, AZ, Canelo, AZ, Animas, NM, and Orogrande, NM (data from wrcc.dri.edu, accessed 2022), which are close to the fossil localities that show the highest $C_4/(C_4+C_3)$ in Connin et al. (1998) and Metcalfe et al. (2011), these equations predict modern %C_4 of 55–70% (Table 3), which fall within the range of %C_4 in modern sites nearby (30–75%; Paruelo and Lauenroth, 1996).

To model C_4 grass abundances under Pleistocene conditions, we followed Connin et al. (1998) by increasing MAP by 50%, and decreasing mean annual temperature by 6 °C. If we maintain modern summer precipitation rates (which implies a decrease in JJA/MAP), the model of Paruelo and Lauenroth (1996) predicts absolute %C_4 abundances of 30–45% of total plant biomass (Table 3). To increase absolute %C_4 abundances to ~50% (median) or 70–80% (extreme), an increase in summer precipitation of ~20–50% (median) to 50–100% (extreme) would be necessary (Table 3) – this is essentially the isotopic justification for increased summer precipitation. However, because grazers eat grass, the calculation of %C_4 should not be for absolute C_4 abundance across the landscape, but rather for the proportion of C_4 to C_4+C_3 grasses. To our knowledge, C_3 grass abundances have not been calculated, so predicted grass $C_4/(C_4+C_3)$ under Pleistocene conditions is as yet unknown.

Considering modern ecosystems (shrubland ecosystems), predicted abundances of C_3 grasses in southern Arizona and New Mexico are ~0% (Table 3), consistent with floral surveys (Paruelo and Lauenroth, 1996). Consequently, a grazer there today would be expected to show high %C_4 (from grass proportions) even though observed %C_4 across the landscape is as low as 30% (Paruelo and Lauenroth, 1996). If grazers consume some (C_3) herbs and shrubs, %C_4 might be less than 100%. However, horses and bison in the region consume 80–100% grass (van Vuren, 1984; Scasta et al., 2016), so %C_4 should be high.

To predict C_3 grass abundance under late Pleistocene conditions, we assume the same changes as Connin et al. (1998) for mean annual temperature (6 °C lower) and MAP (50% higher). If we assume summer precipitation remained the same as today (implying lower JJA/MAP), and that the habitat is grassland, not shrubland (an assumption that maximizes calculated %C_3), predicted %C_3 and %C_4 grasses are similar (30–45%), with grass $C_4/(C_4+C_3)$ ~45–55% (Table 3). If a shrubland ecosystem is assumed, calculated $C_4/(C_4+C_3)$ is 70–80% (Table 3). Because we do not know whether Pleistocene herbivores occupied grasslands or shrublands, these calculations indicate that no increase in summer precipitation is required to explain herbivore tooth enamel $\delta^{13}C$ values. The median value of 50%C_4 for the late Pleistocene is consistent with grassland ecosystems, while the maximum value of 70–80% C_4 is consistent with either shrublands or with seasonal consumption of C_4 grass. However, it is worth considering interpretations of C_4 grassland ecosystems derived from paleosol and packrat midden records (section 7.5.2), and whether other factors besides summer precipitation, such as lower p_{CO2}, might be able to sustain higher proportions of C_4 grasses.

Table 3
Models of C_3 and C_4 grass abundances.

Location	MAT (°C)	MAP (mm)	JJA (mm)	JJA/MAP	DJF (mm)	DJF/MAP	Biome	%C_4	%C_3	$C_4/(C_3+C_4)$
Modern data										
Animas, NM	16	276	126	0.46	53	0.19	shrubland	54.8	0.0	1.00
Orogrande, NM	17	224	111	0.50	37	0.16	shrubland	58.8	0.0	1.00
Benson, AZ	17	288	149	0.52	54	0.19	shrubland	65.3	0.0	1.00
Elgin, AZ	14	463	235	0.51	97	0.21	shrubland	69.3	2.9	0.96
Pleistocene climate: MAT − 6 °C; no pCO2 effect; MAP + 50%; modern JJA; grassland biome										
Animas, NM	10	414	126	0.30	79	0.19	grassland	29.7	36.7	0.45
Orogrande, NM	11	336	111	0.33	55	0.16	grassland	31.3	30.9	0.50
Benson, AZ	11	432	149	0.34	81	0.19	grassland	38.8	33.4	0.54
Elgin, AZ	8	694	235	0.34	146	0.21	grassland	45.0	44.2	0.50
Pleistocene climate: MAT − 6 °C; no pCO2 effect; MAP + 50%; JJA + 100%; grassland biome										
Animas, NM	10	414	251	0.61	79	0.19	grassland	70.8	36.7	0.66
Orogrande, NM	11	336	222	0.66	55	0.16	grassland	76.0	30.9	0.71
Benson, AZ	11	432	297	0.69	81	0.19	grassland	85.3	33.4	0.72
Elgin, AZ	8	694	469	0.68	146	0.21	grassland	90.7	44.2	0.67
Pleistocene climate: MAT − 6 °C; no pCO2 effect; MAP + 50%; modern JJA; shrubland biome										
Animas, NM	10	414	126	0.30	79	0.19	shrubland	29.7	12.8	0.70
Orogrande, NM	11	336	111	0.33	55	0.16	shrubland	31.3	7.1	0.81
Benson, AZ	11	432	149	0.34	81	0.19	shrubland	38.8	9.6	0.80
Elgin, AZ	8	694	235	0.34	146	0.21	shrubland	45.0	20.4	0.69
Pleistocene climate: MAT − 6 °C; T_x + 5 °C; MAP + 50%; modern JJA; grassland biome										
Animas, NM	15	414	126	0.30	79	0.19	grassland	40.7	22.1	0.65
Orogrande, NM	16	336	111	0.33	55	0.16	grassland	41.4	16.4	0.72
Benson, AZ	16	432	149	0.34	81	0.19	grassland	49.0	18.9	0.72
Elgin, AZ	13	694	235	0.34	146	0.21	grassland	58.1	29.6	0.66
Pleistocene climate: MAT − 6 °C; T_x + 9 °C; MAP + 50%; modern JJA; grassland biome										
Animas, NM	19	414	126	0.30	79	0.19	grassland	47.1	10.5	0.82
Orogrande, NM	20	336	111	0.33	55	0.16	grassland	47.5	4.8	0.91
Benson, AZ	20	432	149	0.34	81	0.19	grassland	55.0	7.3	0.88
Elgin, AZ	17	694	235	0.34	146	0.21	grassland	65.4	18.0	0.78

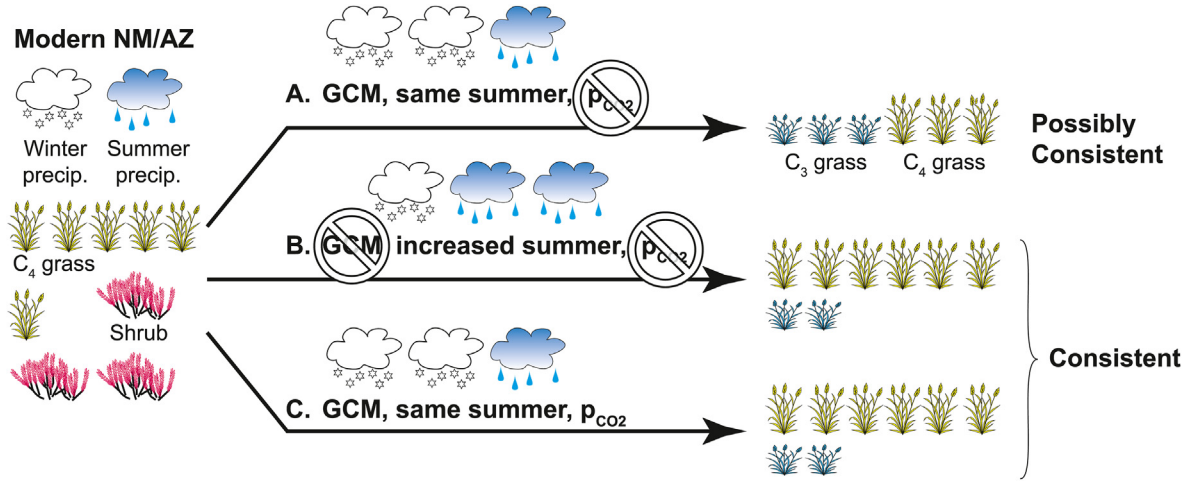

Fig. 8. Comparison of hypotheses regarding summer vs. winter precipitation amounts and effects of p_{CO2} on proportions of C_3 vs. C_4 grasses during the latest Pleistocene in New Mexico (NM) and Arizona (AZ). Left side shows modern proportions of winter vs. summer precipitation and relative abundances of C_4 grass and shrubs. (A) Assuming GCMs are correct with increased winter precipitation but similar summer precipitation, ignoring p_{CO2} effects. Predicted abundances of C_3 and C_4 grasses are approximately equal, consistent with some but not all isotopic and floral data. (B) Ignoring GCMs, assuming enhanced summer precipitation, and ignoring p_{CO2} effects. Predicted abundances of C_3 and C_4 grasses are consistent with isotopic and floral data. (C) Assuming GCMs are correct and accounting for p_{CO2} effects. Predicted abundances of C_3 and C_4 grasses are consistent with isotopic and floral data.

7.5.2. Evaluating paleosol $\delta^{13}C$ and packrat midden records in the context of lower p_{CO2}

Floral macrofossils in late Pleistocene packrat middens from southernmost Arizona and New Mexico are dominated by trees, C_4 grasses, and summer-flowering herbs, while desert shrubs do not become abundant until after ~5 ka (Holmgren et al., 2007). Holmgren et al. (2007) interpreted these data to indicate late Pleistocene C_4 grasslands, stabilized by abundant summer rain. High $\delta^{13}C$ values for late Pleistocene paleosol carbonate in southernmost New Mexico (Monger et al., 1998) were also interpreted to indicate C_4 grasslands (Buck and Monger, 1999). However, these studies did not consider directly the effect of p_{CO2} on the stability of C_4 vs. C_3 grasses. Accounting for p_{CO2} further reinforces the conclusion that enhanced summer precipitation may not be needed to explain late Pleistocene floras and isotope records.

In general, C_4 grasses should be more competitive with C_3 plants under low p_{CO2} conditions (e.g., Ehleringer, 1978; Ehleringer et al., 1997; Collatz et al., 1998; Sage, 2004) that occurred during the late Pleistocene. This effect can be described in terms of a crossover temperature (T_x), which is the temperature at which, for a specified CO_2 level, C_3 and C_4 plants are photosynthetically equivalent (Ehleringer et al., 1997). C_4 plants are more competitive at higher temperatures, but decreasing p_{CO2} decreases T_x. For example, equations from Collatz et al. (1998) predict that at pre-industrial p_{CO2} = 280 ppmv (parts per million by volume), T_x = 18 °C, whereas at latest Pleistocene p_{CO2} = 200 ppmv (e.g., see summary of Eggleston et al., 2016), T_x = 12 °C. That is, the temperature at which C_3 and C_4 plants are photosynthetically equivalent decreases by ΔT_x = 6 °C as p_{CO2} decreases from 280 to 200 ppmv. This ΔT_x can be accounted for by increasing the temperature used in predictive equations. Adding ΔT_x to estimated paleotemperatures in the equations of Paruelo and Lauenroth (1996) accounts for changing p_{CO2} levels over time (Kohn and McKay, 2012), at least for calculated abundances of C_3 and C_4 grasses.

Some ambiguities accompany the assignment of an appropriate ΔT_x because of modern increases in p_{CO2}. Floral observations used to develop predictive equations were collected in the late 20th century, when p_{CO2} = 350 ppmv. However, floras might not respond immediately to p_{CO2}, so reflect pre-industrial conditions when p_{CO2} = 280 ppmv. Relative to p_{CO2} = 200–230 ppmv (15–50 ka; e.g., Petit et al., 1999), these alternatives correspond to ΔT_x of ~ 5–10 °C. Applying this correction to the equations of Paruelo and Lauenroth (1996) to Pleistocene conditions increases predicted $\%C_4$ to 60–70%, decreases $\%C_3$ to 5–30% (assuming grasslands), and increases $C_4/(C_4+C_3)$ to ~65–90% (Table 3). Late Pleistocene shrubland ecosystems would have $\%C_3 \leq 5\%$ and $C_4/(C_4+C_3)$ ~90–100% (Table 3). These calculations imply that decreases in p_{CO2} could readily explain the development of C_4 grasslands in the southwestern U.S. during the late Pleistocene without the need for invoking increased summer precipitation under cooler conditions. This result reinforces the conclusions of Cotton et al. (2016) that stability of C_4 grasses during the Pleistocene reflected low p_{CO2}.

Although we cannot quantitatively reevaluate late Pleistocene temperatures and precipitation, our data and calculations provide new directions for refining past proxy estimates (Fig. 8). Past estimates of temperature and precipitation based on macroflora and pollen (e.g., see summary of Bartlein et al., 2011) should be reconsidered in light of the effect of p_{CO2} on plant stability and water usage. For example, anthropogenic increases in p_{CO2} have increased water use efficiency (e.g., Keenan et al., 2013; Mathias and Thomas, 2021) at least in part because increased p_{CO2} reduces the need for either densely spaced or fully open stomata, which decreases evaporative water loss. Thus, water requirements for some plant species today, under elevated p_{CO2}, are less than in the past. In the late Pleistocene, when p_{CO2} was lower, water requirements likely were higher. Consequently, estimates of late Pleistocene MAP may be generally too low – Pleistocene plants needed to transpire more water in a low p_{CO2} environment, so MAP likely was higher than calculated. Conversely, in the context of C_3–C_4 competition, C_4 plants should have been stable at lower temperatures than their modern counterparts. To outcompete C_4 plants, C_3 plants require lower temperatures, suggesting MAT may have been lower than calculated.

8. Conclusions

The Las Vegas Formation represents an unusually complete and highly resolved sequence of paleowetland deposits that spans the middle-late Pleistocene and early Holocene. Inset within these deposits are vertebrate remains of the Tule Springs local fauna that

date to between ~100 and 12.5 ka. Tooth enamel of *Equus*, *Bison*, *Mammuthus*, and *Camelops* from this fauna were used to evaluate competing models of the seasonality and source of precipitation that supported large pluvial lakes and extensive springs and wetlands throughout the western and southwestern U.S. during the late Pleistocene.

Low tooth enamel $\delta^{18}O$ values for grazers (*Equus*, *Bison*, and *Mammuthus*) compared to modern horses reflect an increased proportion of winter precipitation, which is consistent with GCMs that predict the enhanced precipitation that fell during the late Pleistocene resulted from a southward shift of wintertime westerlies and was sourced from the northern Pacific (the SOW model). High tooth enamel $\delta^{13}C$ values for these same grazing herbivores indicate they consumed a higher proportion of C_4 grasses than horses today, but substantially less than modern proportions of C_4 grasses across the landscape. We hypothesize this disparity reflects niche partitioning and dietary competition, such that modern horses can selectively feed on C_3 vegetation more so than their Pleistocene counterparts, who were competing for resources with far more taxa. In addition, increases in $C_4/(C_4+C_3)$ in Pleistocene grazer diet in the Las Vegas Valley and elsewhere in the southwestern U.S. can be explained by lower p_{CO2}, rather than an increase in proportions or amounts of summer precipitation (Fig. 8). Together, our data and interpretations suggest that Pleistocene temperatures and precipitation derived from floral records should be reevaluated in the context of the effects of niche partitioning and p_{CO2} on the stability of C_3 vs. C_4 plants, in addition to the usual winter vs. summer precipitation regimes.

Author contributions

All authors made substantial contributions to the research and writing/editing. Conceptualization: KBS, JSP, ES, MJK. Methodology: MJK, KBS, JSP, LMR. Data collection, validation, and analysis: MJK, LMR, JC, AD. Writing: all authors. Visualization: MJK, KBS, JSP, AD. Supervision: MJK, KBS, JSP, LMR. Funding acquisition: MJK, KBS, JSP.

Declaration of competing interest

The authors declare that they have no known competing financial interests or personal relationships that could have appeared to influence the work reported in this paper.

Data availability

Data will be included as tables in the article. Also, a USGS link provides access to all data. Link is provided in the text.

Acknowledgements

Specimens for this project were collected with funding through BLM Federal Assistance Agreement L08AC13098 (KBS). Other funding includes NSF grants EAR0842367 and EAR1561027 (MJK) and the U.S. Geological Survey Climate and Land Use Change Research and Development Program through the Quaternary Hydroclimate Records of Spring Ecosystems project (KBS/JSP). Any use of trade, firm, or product names is for descriptive purposes only and does not imply endorsement by the U.S. Government. Downloadable files of the data presented in the text and Supplementary Information can be found at https://doi.org/10.5066/P9DBH6V7. We thank Sam Evans for support collecting initial isotopic data, Dan Muhs, Natalie Latysh, Bruce MacFadden, and an anonymous reviewer for constructive reviews of this manuscript, and Tabitha Romero, Erin Eichenberg, and Lauren Perry for providing modern specimens of *Equus* teeth. We greatly appreciate the U.S. National Park Service staff of Tule Springs Fossil Beds National Monument for continuing to facilitate our work under permit TUSK-2015-2019SCI-001 (KBS, Principal Investigator).

Appendix A. Supplementary data

Supplementary data to this article can be found online at https://doi.org/10.1016/j.quascirev.2022.107784.

References

Alder, J.R., Hostetler, S.W., 2015. Global climate simulations at 3000-year intervals for the last 21 000 years with the GENMOM coupled atmosphere-ocean model. Clim. Past 11, 449–471. https://doi.org/10.5194/cp-11-449-2015.

Andersen, K.K., Svensson, A., Johnsen, S.J., Rasmussen, S.O., Bigler, M., Röthlisberger, R., Ruth, U., Siggaard-Andersen, M.-L., Peder Steffensen, J., Dahl-Jensen, D., 2006. The Greenland Ice Core Chronology 2005, 15–42ka. Part 1: constructing the time scale. Quat. Sci. Rev. 25, 3246–3257. https://doi.org/10.1016/j.quascirev.2006.08.002.

Asmerom, Y., Polyak, V.J., Burns, S.J., 2010. Variable winter moisture in the southwestern United States linked to rapid glacial climate shifts. Nat. Geosci. 3, 114–117.

Ayliffe, L.K., Chivas, A.R., 1990. Oxygen isotope composition of the bone phosphate of Australian kangaroos: potential as a palaeoenvironmental recorder. Geochim. Cosmochim. Acta 54, 2603–2609.

Ayliffe, L.K., Chivas, A.R., Leakey, M.G., 1994. The retention of primary oxygen isotope compositions of fossil elephant skeletal phosphate. Geochim. Cosmochim. Acta 58, 5291–5298.

Bartlein, P.J., Harrison, S.P., Brewer, S., Connor, S., Davis, B.A.S., Gajewski, K., Guiot, J., Harrison-Prentice, T.I., Henderson, A., Peyron, O., Prentice, I.C., Scholze, M., Seppa, H., Shuman, B., Sugita, S., Thompson, R.S., Viau, A.E., Williams, J., Wu, H., 2011. Pollen-based continental climate reconstructions at 6 and 21 ka: a global synthesis. Clim. Dynam. 37, 775–802. https://doi.org/10.1007/s00382-010-0904-1.

Bell, J.W., Ramelli, A.R., Caskey, S.J., 1998. Geologic map of the Tule springs Park quadrangle, Clark county, Nevada. Nev. Bur. Mines Geol. 113 (1), 24000.

Bell, J.W., Ramelli, A.R., dePolo, C.M., Maldonado, F., Schmidt, D.L., 1999. Geologic map of the Corn Creek springs quadrangle, Clark county, Nevada. Nev. Bur. Mines Geol. 121 (1), 24000.

Benson, L.V., Thompson, R.S., 1987. The physical record of lakes in the Great Basin. In: North America and Adjacent Oceans during the Last Deglaciation, Geology of North America, K-3. Geological Society of America, Boulder, CO, pp. 241–260.

Biasatti, D., Wang, Y., Deng, T., 2010. Strengthening of the East Asian summer monsoon revealed by a shift in seasonal patterns in diet and climate after 2–3Ma in northwest China. Palaeogeogr. Palaeoclimatol. Palaeoecol. 297, 12–25.

Blackwelder, E., 1931. Pleistocene glaciation in the Sierra Nevada and basin and ranges. Geol. Soc. Am. Bull. 42, 865–922.

Bowen, G., 2022. The Online Isotopes in Precipitation Calculator [WWW Document], version 3.1. http://wateriso.utah.edu/waterisotopes/index.html.

Bowen, G.J., Revenaugh, J., 2003. Interpolating the isotopic composition of modern meteoric precipitation. Water Resour. Res. 39. https://doi.org/10.1029/2003WR002086.

Bravo-Cuevas, V.M., Rivals, F., Priego-Vargas, J., 2017. Paleoecology ($\delta^{13}C$ and $\delta^{18}O$ stable isotopes analysis) of a mammalian assemblage from the late Pleistocene of Hidalgo, central Mexico and implications for a better understanding of environmental conditions in temperate North America (18°–36°N Lat.). Palaeogeogr. Palaeoclimatol. Palaeoecol. 485, 632–643. https://doi.org/10.1016/j.palaeo.2017.07.018.

Broecker, W.S., Orr, P.C., 1958. Radiocarbon chronology of lake Lahontan and lake Bonneville. Geol. Soc. Am. Bull. 69, 1009–1032.

Buck, B.J., Monger, H.C., 1999. Stable isotopes and soil-geomorphology as indicators of Holocene climate change, northern Chihuahuan Desert. J. Arid Environ. 43, 357–373. https://doi.org/10.1006/jare.1999.0584.

Cerling, T.E., Harris, J.M., 1999. Carbon isotope fractionation between diet and bioapatite in ungulate mammals and implications for ecological and paleoecological studies. Oecologia 120, 347–363.

Cerling, T.E., Harris, J.M., MacFadden, B.J., Leakey, M.G., Quade, J., Eisenmann, V., Ehleringer, J.R., 1997. Global vegetation change through the Miocene/Pliocene boundary. Nature 389, 153–158.

Clementz, M.T., 2012. New insight from old bones: stable isotope analysis of fossil mammals. J. Mammal. 93, 368–380.

COHMAP Members, 1988. Climatic changes of the last 18,000 years: observations and model simulations. Science 241, 1043–1052.

Collatz, G.J., Berry, J.A., Clark, J.S., 1998. Effects of climate and atmospheric CO_2 partial pressure on the global distribution of C_4 grasses: present, past, and future. Oecologia 114, 441–454.

Connin, S.L., Betancourt, J., Quade, J., 1998. Late Pleistocene C_4 plant dominance and summer rainfall in the southwestern US from isotopic study of herbivore teeth. Quat. Res. 50, 179–193.

Cotton, J.M., Cerling, T.E., Hoppe, K.A., Mosier, T.M., Still, C.J., 2016. Climate, CO_2, and

the history of north American grasses since the last glacial maximum. Sci. Adv. 2, e1501346. https://doi.org/10.1126/sciadv.1501346.
Crowley, B.E., Koch, P.L., Davis, E.B., 2008. Stable isotope constraints on the elevation history of the Sierra Nevada Mountains, California. Geol. Soc. Am. Bull. 120, 588–598. https://doi.org/10.1130/B26254.1.
Dansgaard, W., 1964. Stable isotopes in precipitation. Tellus 16, 436–468.
Dalton, A.S., Margold, M., Stokes, C.R., Tarasov, L., Dyke, A.S., Adams, R.S., Allard, S., Arends, H.E., Atkinson, N., Attig, J.W., Barnett, P.J., Barnett, R.L., Batterson, M., Bernatchez, P., Borns Jr., H.W., Breckenridge, A., Briner, J.P., Brouard, E., Campbell, J.E., Carlson, A.E., Clague, J.J., Curry, B.B., Daigneault, R.-A., Dobé-Loubert, H., Easterbrook, D.J., Franzi, D.A., Friedrich, H.G., Funder, S., Gauthier, M.S., Gowan, A.S., Harris, K.L., Hétu, B., Hooyer, T.S., Jennings, C.E., Johnson, M.D., Kehew, A.E., Kelley, S.E., Kerr, D., King, E.L., Kjeldsen, K.K., Knaeble, A.R., Lajeunesse, P., Lakeman, T.R., Lamothe, M., Larson, P., Lavoie, M., Loope, H.M., Lowell, T.V., Lusardi, B.A., Manz, L., McMartin, I., Nixon, F.C., Occhietti, S., Parkhill, M.A., Piper, D.J.W., Pronk, A.G., Richard, P.J.H., Ridge, J.C., Ross, M., Roy, M., Seaman, A., Shaw, J., Stea, R.R., Teller, J.T., Thompson, W.B., Thorleifsen, L.H., Utting, D.J., Veillette, J.J., Ward, B.C., Weddle, T.K., Wright Jr., H.E., 2020. An updated radiocarbon-based ice margin chronology for the last deglaciation of the North American Ice Sheet Complex. Quat. Sci. Rev. 234, 106223. https://doi.org/10.1016/j.quascirev.2020.106223.
DeNiro, M.J., Epstein, S., 1978. Influence of diet on the distribution of carbon isotopes in animals. Geochim. Cosmochim. Acta 42, 495–506.
DeSantis, L.R.G., Feranec, R.S., MacFadden, B.J., 2009. Effects of global warming on ancient mammalian communities and their environments. PLoS One 4 (6), e5750. https://doi.org/10.1371/journal.pone.0005750.
Diefendorf, A.F., Mueller, K.E., Wing, S.L., Koch, P.L., Freeman, K.H., 2010. Global patterns in leaf ^{13}C discrimination and implications for studies of past and future climate. Proc. Natl. Acad. Sci. 107, 5738–5743.
Eggleston, S., Schmitt, J., Bereiter, B., Schneider, R., Fischer, H., 2016. Evolution of the stable carbon isotope composition of atmospheric CO_2 over the last glacial cycle. Paleoceanography 31, 434–452. https://doi.org/10.1002/2015PA002874.
Ehleringer, J.R., 1978. Implications of quantum yield differences to the distributions of C_3 and C_4 grasses. Oecologia 31, 255–267.
Ehleringer, J.R., Cerling, T.E., Helliker, B.R., 1997. C_4 photosynthesis, atmospheric CO_2 and climate. Oecologia 112, 285–299.
Feranec, R.S., MacFadden, B.J., 2000. Evolution of the grazing niche in Pleistocene mammals from Florida: evidence from stable isotopes. Palaeogeogr. Palaeoclimatol. Palaeoecol. 162, 155–169.
Feranec, R.S., Hadly, E.A., Paytan, A., 2009. Stable isotopes reveal seasonal competition for resources between late Pleistocene bison (Bison) and horse (Equus) from Rancho La Brea, southern California. Palaeogeogr. Palaeoclimatol. Palaeoecol. 271, 153–160.
Francey, R.J., Allison, C.E., Etheridge, D.M., Trudinger, C.M., Enting, I.G., Leuenberger, M., Langenfelds, R.L., Michel, E., Steele, L.P., 1999. A 1000–year high precision record of $\delta^{13}C$ in atmospheric CO_2. Tellus Ser. B Chem. Phys. Meteorol. 51B, 170–193.
Fricke, H.C., Clyde, W.C., O'Neil, J.R., 1998. Intra–tooth variations in $\delta^{18}O(PO4)$ of mammalian tooth enamel as a record of seasonal variations in continental climate variables. Geochim. Cosmochim. Acta 62, 1839–1850.
Fricke, H.C., O'Neil, J.R., 1996. Inter-and intra-tooth variation in the oxygen isotope composition of mammalian tooth enamel phosphate; implications for palaeoclimatological and palaeobiological research. Palaeogeogr. Palaeoclimatol. Palaeoecol. 126, 91–99.
Friedman, I., 2000. Database of Surface and Ground Water Samples Analyzed for Deuterium and Oxygen-18 from the Western States of Arizona, California, Colorado, Idaho, Montana, Nevada, New Mexico, Oregon, Utah, Washington, and Wyoming. United States Geological Survey Open-File. Report 00–388.
Gat, J.R., 1996. Oxygen and hydrogen isotopes in the hydrologic cycle. Annu. Rev. Earth Planet Sci. 24, 225–262.
Gilbert, G.K., 1890. Lake Bonneville, vol. 1. United States Geological Survey Monograph, p. 438.
Goldstein, H.L., Springer, K.B., Pigati, J.S., Reheis, M.C., Skipp, G.L., 2021. Aeolian sediments in paleowetland deposits of the las Vegas Formation. Quat. Res. 104, 1–13.
Graven, H., Allison, C.E., Etheridge, D.M., Hammer, S., Keeling, R.F., Levin, I., Meijer, H.A.J., Rubino, M., Tans, P.P., Trudinger, C.M., Vaughn, B.H., White, J.W.C., 2017. Compiled records of carbon isotopes in atmospheric CO_2 for historical simulations in CMIP6. Geosci. Model Dev. 10, 4405–4417. https://doi.org/10.5194/gmd-10-4405-2017.
Grootes, P.M., Stuiver, M., 1997. Oxygen 18/16 variability in Greenland snow and ice with 10^{-3} to 10^{5}-year resolution. J. Geophys. Res. 102, 26455–26470.
Harrill, J.R., 1976. Pumping and groundwater storage depletion in las Vegas Valley, Nevada, 1955-1974. Water Resour. Bull. 44, 70. Nevada Department of Conservation and Natural Resources.
Harris, E.B., Kohn, M.J., Strömberg, C.A., 2020. Stable Isotope Compositions of Herbivore Teeth Indicate Climatic Stability Leading into the Middle Miocene Climatic Optimum, in Idaho, p. 109610. https://doi.org/10.1016/j.palaeo.2020.109610. USA. Palaeogeography, Palaeoclimatology, Palaeoecology.
Haynes Jr., C.V., 1967. Quaternary geology of the Tule springs area, Clark county, Nevada. In: Pleistocene Studies in Southern Nevada. Nevada State Museum of Anthropology, Carson City, NV, pp. 1–104.
Holmgren, C.A., Norris, J., Betancourt, J.L., 2007. Inferences about winter temperatures and summer rains from the late Quaternary record of C_4 perennial grasses and C_3 desert shrubs in the northern Chihuahuan Desert. J. Quat. Sci. 22, 141–161. https://doi.org/10.1002/jqs.1023.
Honke, J.S., Pigati, J.S., Wilson, J., Bright, J., Goldstein, H.L., Skipp, G.L., Reheis, M.C., Havens, J.C., 2019. Late Quaternary paleohydrology of desert wetlands and pluvial lakes in the Soda Lake basin, central Mojave Desert, California (USA). Quat. Sci. Rev. 216, 89–106. https://doi.org/10.1016/j.quascirev.2019.05.021.
Hoppe, K.A., Koch, P.L., 2006. The biogeochemistry of the Aucilla river fauna. In: Webb, S.D. (Ed.), First Floridians and Last Mastodons: the Page-Ladson Site in the Aucilla River. Springer Netherlands, pp. 379–401. https://doi.org/10.1007/978-1-4020-4694-0_13.
Hoppe, K.A., Amundson, R., Vavra, M., McClaran, M.P., Anderson, D.L., 2004. Isotopic analysis of tooth enamel carbonate from modern North American feral horses: implications for paleoenvironmental reconstructions. Palaeogeogr. Palaeoclimatol. Palaeoecol. 203, 299–311.
Hostetler, S.W., Benson, L.V., 1990. Paleoclimatic implications of the high stand of Lake Lahontan derived from models of evaporation and lake level. Clim. Dynam. 4, 207–217.
Iqbal, A., Khan, B.B., 2001. Feeding behaviour of camel...Review. Pak. J. Agric. Sci. 38, 58–63.
Jasechko, S., 2016. Late–Pleistocene precipitation $\delta^{18}O$ interpolated across the global landmass. Geochem. Geophys. Geosyst. 17, 3274–3288. https://doi.org/10.1002/2016GC006400.
Jasechko, S., Lechler, A., Pausata, F.S.R., Fawcett, P.J., Gleeson, T., Cendón, D.I., Galewsky, J., LeGrande, A.N., Risi, C., Sharp, Z.D., Welker, J.M., Werner, M., Yoshimura, K., 2015. Late-glacial to late-Holocene shifts in global precipitation $\delta^{18}O$. Clim. Past 11, 1375–1393. https://doi.org/10.5194/cp-11-1375-2015.
Kadereit, G., Mavrodiev, E.V., Zacharias, E.H., Sukhorukov, A.P., 2010. Molecular phylogeny of Atripliceae (Chenopodioideae, Chenopodiaceae): implications for systematics, biogeography, flower and fruit evolution, and the origin of C_4 photosynthesis. Am. J. Bot. 97, 1664–1687. https://doi.org/10.3732/ajb.1000169.
Keenan, T.F., Hollinger, D.Y., Bohrer, G., Dragoni, D., Munger, J.W., Schmid, H.P., Richardson, A.D., 2013. Increase in forest water-use efficiency as atmospheric carbon dioxide concentrations rise. Nature 499, 324–327. https://doi.org/10.1038/nature12291.
Kim, S.-J., Crowley, T.J., Erickson, D.J., Govindasamy, B., Duffy, P.B., Lee, B.Y., 2008. High-resolution climate simulation of the last glacial maximum. Clim. Dynam. 31, 1–16. https://doi.org/10.1007/s00382-007-0332-z.
Koch, P.L., 1998. Isotopic reconstruction of past continental environments. Annu. Rev. Earth Planet Sci. 26, 573–613.
Koch, P.L., 2007. Isotopic study of the biology of modern and fossil vertebrates. In: Michener, R., Lajtha, K. (Eds.), Stable Isotopes in Ecology and Environmental Science. Blackwell, Boston, pp. 99–154.
Koch, P.L., Tuross, N., Fogel, M.L., 1997. The effects of sample treatment and diagenesis on the isotopic integrity of carbonate in biogenic hydroxylapatite. J. Archaeol. Sci. 24, 417–429.
Koch, P.L., Diffenbaugh, N.S., Hoppe, K.A., 2004. The effects of late Quaternary climate and pCO2 change on C4 plant abundance in the south-central United States. Palaeogeogr. Palaeoclimatol. Palaeoecol. 207, 331–357.
Kohn, M.J., 1996. Predicting animal $\delta^{18}O$: accounting for diet and physiological adaptation. Geochim. Cosmochim. Acta 60, 4811–4829.
Kohn, M.J., 2010. Carbon isotope compositions of terrestrial C_3 plants as indicators of (paleo)ecology and (paleo)climate. Proc. Natl. Acad. Sci. 107, 19691–19695.
Kohn, M.J., Cerling, T.E., 2002. Stable isotope compositions of biological apatite. Rev. Mineral. Geochem. 48, 455–488.
Kohn, M.J., Dettman, D.L., 2007. Paleoaltimetry from stable isotope compositions of fossils. Rev. Mineral. Geochem. 66, 119–154.
Kohn, M.J., Fremd, T.J., 2007. Tectonic controls on isotope compositions and species diversification, John Day Basin, central Oregon. PaleoBios 27, 48–61.
Kohn, M.J., McKay, M.P., 2012. Paleoecology of late Pleistocene–Holocene faunas of eastern and central Wyoming, USA, with implications for LGM climate models. Palaeogeogr. Palaeoclimatol. Palaeoecol. 326–328, 42–53.
Kohn, M.J., Schoeninger, M.J., Valley, J.W., 1998. Variability in oxygen isotope compositions of herbivore teeth: reflections of seasonality or developmental physiology? Chem. Geol. 152, 97–112.
Kohn, M.J., McKay, M.P., Knight, J.L., 2005. Dining in the Pleistocene - who's on the menu? Geology 8, 649–652.
Lachniet, M.S., Denniston, R.F., Asmerom, Y., Polyak, V.J., 2014. Orbital control of western North America atmospheric circulation and climate over two glacial cycles. Nat. Commun. 5, 3805.
Lachniet, M., Asmerom, Y., Polyak, V., Denniston, R., 2017. Arctic cryosphere and Milankovitch forcing of Great Basin paleoclimate. Sci. Rep. 7, 12955. https://doi.org/10.1038/s41598-017-13279-2.
Lachniet, M.S., Asmerom, Y., Polyak, V., Denniston, R., 2020. Great Basin paleoclimate and aridity linked to Arctic warming and tropical pacific sea surface temperatures. Paleoceanogr. Paleoclimatol. 35. https://doi.org/10.1029/2019PA003785.
Levin, N.E., Cerling, T.E., Passey, B.H., Harris, J.M., Ehleringer, J.R., 2006. A stable isotope aridity index for terrestrial environments. Proc. Natl. Acad. Sci. 103, 11201–11205.
Longwell, C.R., Pampeyan, E.H., Bower, B., Roberts, R.J., 1965. Geology and Mineral Deposits of Clark County, Nevada, vol. 62. Nevada Bureau of Mines and Geology Bulletin, pp. 1–218.
Lundstrom, S.C., Page, W.R., Langenhaim, V.E., Young, O.D., Mahan, S.A., Dixon, G.L., 1998. Preliminary Geologic Map of the Valley Quadrangle, Clark County, Nevada. United States Geological Survey. Open-File Report No. 98–508. https://pubs.er.usgs.gov/publication/ofr98508.

Luz, B., Cormie, A.B., Schwarcz, H.P., 1990. Oxygen isotope variations in phosphate of deer bones. Geochim. Cosmochim. Acta 54, 1723–1728.
Lyle, M., Heusser, L., Ravelo, C., Yamamoto, M., Barron, J., Diffenbaugh, N.S., Herbert, T., Andreasen, D., 2012. Out of the tropics: the Pacific, Great Basin lakes, and late Pleistocene water cycle in the western United States. Science 337, 1629–1633.
MacFadden, B.J., 2000. Cenozoic mammalian herbivores from the Americas: reconstructing ancient diets and terrestrial communities. Annu. Rev. Ecol. Syst. 31, 33–59.
MacFadden, B.J., Cerling, T.E., 1996. Mammalian herbivore communities, ancient feeding ecology, and carbon isotopes: a 10 million-year sequence from the Neogene of Florida. J. Vertebr. Paleontol. 16, 103–115.
Mathias, J.M., Thomas, R.B., 2021. Global tree intrinsic water use efficiency is enhanced by increased atmospheric CO_2 and modulated by climate and plant functional types. Proc. Natl. Acad. Sci. 118, e2014286118. https://doi.org/10.1073/pnas.2014286118.
Mawby, J.E., 1967. Fossil vertebrates of the Tule springs site, Nevada. In: Wormington, H.M., Ellis, D. (Eds.), Pleistocene Studies in Southern Nevada, Nevada State Museum Anthropological Papers 13, pp. 105–128.
Metcalfe, J.Z., Longstaffe, F.J., Ballenger, J.A.M., Haynes, C.V., 2011. Isotopic paleoecology of Clovis mammoths from Arizona. Proc. Natl. Acad. Sci. 108, 17916–17920. https://doi.org/10.1073/pnas.1113881108.
Mifflin, M.D., Wheat, M.M., 1979. Pluvial lakes and estimated pluvial climates of Nevada. Nev. Bur. Mines Geol. Bull. 94, 1–57.
Monger, H.C., Cole, D.R., Gish, J.W., Giordano, T.H., 1998. Stable carbon and oxygen isotopes in Quaternary soil carbonates as indicators of ecogeomorphic changes in the northern Chihuahuan Desert, USA. Geoderma 82, 137–172. https://doi.org/10.1016/S0016-7061(97)00100-6.
Page, W.R., Lundstrom, S.C., Harris, A.G., Langenheim, V.E., Workman, J.B., Mahan, S.A., Paces, J.B., Dixon, G.L., Rowley, P.D., Burchfiel, B.C., Bell, J.W., Smith, E.I., 2005. Geologic and Geophysical Maps of the Las Vegas 30'x60' Quadrangle, Clark and Nye Counties, Nevada, and Inyo Country, vol. 2814. United States Geological Survey Scientific Investigations Map, California. https://pubs.usgs.gov/sim/2005/2814/.
Pardi, M.I., DeSantis, L.R.G., 2021. Dietary plasticity of North American herbivores: a synthesis of stable isotope data over the past 7 million years. Proc. R. Soc. B 288, 20210121. https://doi.org/10.1098/rspb.2021.0121.
Paruelo, J.M., Lauenroth, W.K., 1996. Relative abundance of plant functional types in grasslands and shrublands of North America. Ecol. Appl. 6, 1212–1224.
Passey, B.H., Robinson, T.F., Ayliffe, L.K., Cerling, T.E., Sponheimer, M., Dearing, M.D., Roeder, B.L., Ehleringer, J.R., 2005. Carbon isotope fractionation between diet, breath CO_2, and bioapatite in different mammals. J. Archaeol. Sci. 32, 1459–1470.
Peng, C.H., Guiot, J., Van Campo, E., 1998. Estimating changes in terrestrial vegetation and carbon storage: using palaeoecological data and models. Quat. Sci. Rev. 17, 719–735.
Pérez-Crespo, V.A., Arroyo-Cabrales, J., Alva-Valdivia, L.M., Morales-Puente, P., Cienfuegos-Alvarado, E., 2012a. Diet and habitat definitions for Mexican glyptodonts from Cedral (San Luis Potosí, México) based on stable isotope analysis. Geol. Mag. 149, 153–157. https://doi.org/10.1017/S0016756811000951.
Pérez-Crespo, V.A., Arroyo-Cabrales, J., Alva-Valdivia, L.M., Morales-Punte, P., Cienfuegos-Alvarado, E., 2012b. Datos isotópicos ($\delta^{13}C$, $\delta^{18}O$) de la fauna pleistocenica de la Laguna de las Cruces, San Luis Potosí, México. Rev. Mex. Ciencias Geol. 29, 299–307.
Petit, J.R., Jouzel, J., Raynaud, D., Barkov, N.I., Barnola, J.M., Basile, I., Bender, M., Chappellaz, J., Davis, M., Delaygue, G., Delmotte, M., Kotlyakov, V.M., Legrand, M., Lipenkov, V.Y., Lorius, C., Pepin, L., Ritz, C., Saltzman, E., Stievenard, M., 1999. Climate and atmospheric history of the past 420,000 years from the Vostok ice core, Antarctica. Nature 399, 429–436.
Pigati, J.S., Bright, J.E., Shanahan, T.M., Mahan, S.A., 2009. Late Pleistocene paleohydrology near the boundary of the Sonoran and Chihuahuan deserts, southeastern Arizona, USA. Quat. Sci. Rev. 28, 286–300. https://doi.org/10.1016/j.quascirev.2008.09.022.
Pigati, J.S., Miller, D.M., Bright, J.E., Mahan, S.A., Nekola, J.C., Paces, J.B., 2011. Chronology, sedimentology, and microfauna of groundwater discharge deposits in the central Mojave Desert, Valley Wells, California. Geol. Soc. Am. Bull. 123, 2224–2239. https://doi.org/10.1130/B30357.1.
Quade, J., 1986. Late quaternary environmental changes in the upper las Vegas Valley, Nevada. Quat. Res. 26, 340–357. https://doi.org/10.1016/0033-5894(86)90094-3.
Quade, J., Pratt, W.L., 1989. Late Wisconsin groundwater discharge environments of the southwestern Indian Springs Valley, southern Nevada. Quat. Res. 31, 351–370.
Quade, J., Mifflin, M.D., Pratt, W.L., McCoy, W., 1995. Fossil spring deposits in the southern Great Basin and their implications for changes in water-table levels near Yucca Mountain, Nevada, during Quaternary time. Geol. Soc. Am. Bull. 107, 213–230.
Quade, J., Forester, R.M., Pratt, W.L., Carter, C., 1998. Black mats, spring-fed streams, and late-Glacial-age recharge in the southern Great Basin. Quat. Res. 49, 129–148. https://doi.org/10.1006/qres.1997.1959.
Quade, Forester, R.M., Whelan, J.F., 2003. Late Quaternary Paleohydrologic and Paleotemperature Change in Southern Nevada, vol. 368. Geological Society of America Special Paper, pp. 165–188.
Ramelli, A.R., Page, W.R., Manker, C.R., Springer, K.B., 2011. Geologic map of the Gass Peak SW quadrangle, Clark county, Nevada. Nev. Bur. Mine. Geol. Map 175, 1:24,000.
Ramelli, A.R., Page, W.R., Manker, C.R., Springer, K.B., 2012. Preliminary Geologic Map of the Corn Creek Springs NW Quadrangle, Clark County, Nevada. Nevada Bureau of Mines and Geology Open-File. Report No. 12–7. 1:24,000.
Reheis, M., 1999. Highest Pluvial-Lake Shorelines and Pleistocene climate of the western Great Basin. Quat. Res. 52, 196–205. https://doi.org/10.1006/qres.1999.2064.
Reimer, P.J., Austin, W.E.N., Bard, E., Bayliss, A., Blackwell, P.G., Bronk Ramsey, C., Butzin, M., Cheng, H., Edwards, R.L., Friedrich, M., Grootes, P.M., Guilderson, T.P., Hajdas, I., Heaton, T.J., Hogg, A.G., Hughen, K.A., Kromer, B., Manning, S.W., Muscheler, R., Palmer, J.G., Pearson, C., van der Plicht, J., Reimer, R.W., Richards, D.A., Scott, E.M., Southon, J.R., Turney, C.S.M., Wacker, L., Adolphi, F., Büntgen, U., Capano, M., Fahrni, S.M., Fogtmann-Schulz, A., Friedrich, R., Köhler, P., Kudsk, S., Miyake, F., Olsen, J., Reinig, F., Sakamoto, M., Sookdeo, A., Talamo, S., 2020. The IntCal20 Northern Hemisphere radiocarbon age calibration curve (0–55 cal kBP). Radiocarbon 62, 725–757. https://doi.org/10.1017/RDC.2020.41.
Rozanski, K., Araguas-Araguas, L., Gonfiantini, R., 1993. Isotopic patterns in modern global precipitation. In: Swart, P.K., Lohmann, K.C., McKenzie, J.A., Savin, S. (Eds.), Climate Change in Continental Isotopic Records, Geophysical Monograph. American Geophysical Union, Washington, pp. 1–36.
Russell, I.C., 1885. Geological History of Lake Lahontan, a Quaternary Lake of Northwestern Nevada, vol. 11. United State Geological Survey Monograph, p. 288.
Sage, R.F., 2004. The evolution of C_4 photosynthesis. New Phytol. 161, 341–370.
Sarangi, V., Agrawal, S., Sanyal, P., 2021. The disparity in the abundance of C_4 plants estimated using the carbon isotopic composition of paleosol components. Palaeogeogr. Palaeoclimatol. Palaeoecol. 561, 110068.
Scasta, J.D., Beck, J.L., Angwin, C.J., 2016. Meta-Analysis of diet composition and potential conflict of wild horses with livestock and wild ungulates on western rangelands of North America. Rangel. Ecol. Manag. 69, 310–318. https://doi.org/10.1016/j.rama.2016.01.001.
Schmidt-Nielsen, B., Schmidt-Nielsen, K., Houpt, T.R., Jarnum, S.A., 1956. Water balance of the camel. Am. J. Physiol. 185, 185–194.
Scott, E., Springer, K.B., Sagebiel, J.C., 2017. The Tule springs local fauna: Rancholabrean vertebrates from the las Vegas Formation, Nevada. Quat. Int. 443, 105–121. https://doi.org/10.1016/j.quaint.2017.06.001.
Semprebon, G.M., Rivals, F., 2010. Trends in the paleodietary habits of fossil camels from the Tertiary and Quaternary of North America. Palaeogeogr. Palaeoclimatol. Palaeoecol. 295, 131–145.
Shanahan, S.A., Silverman, D., Ehrenberg, A., 2007. Land Cover Types of the Las Vegas Wash, Nevada. Las Vegas Wash Coordination Committee, p. 42. https://digitalscholarship.unlv.edu/water_pubs/112.
Snyder, C.T., Hardman, G., Zdenek, F.F., 1964. Pleistocene Lakes in the Great Basin. Nevada Bureau of Mines and Geology. Map I-416, 1:1,000,000.
Springer, K.B., Pigati, J.S., 2020. Climatically driven displacement on the Eglington fault, las Vegas, Nevada, USA. Geology 48, 574–578. https://doi.org/10.1130/G47162.1.
Springer, K.B., Manker, C.R., Pigati, J.S., 2015. Dynamic response of desert wetlands to abrupt climate change. Proc. Natl. Acad. Sci. 112, 14522–14526. https://doi.org/10.1073/pnas.1513352112.
Springer, K.B., Pigati, J.S., Manker, C.R., Mahan, S.A., 2018. The Las Vegas Formation. United States Geological Survey, p. 62. Professional Paper 1839.
Street-Perrott, F.A., Huang, Y., Perrott, R.A., Eglinton, G., Barker, P., Khelifa, L.B., Harkness, D.D., Olago, D.O., 1997. Impact of lower atmospheric carbon dioxide on tropical mountain ecosystems. Science 278, 1422–1426.
Tejada-Lara, J.V., MacFadden, B.J., Bermudez, L., Rojas, G., Salas-Gismondi, R., Flynn, J.J., 2018. Body mass predicts isotope enrichment in herbivorous mammals. Proc. R. Soc. B 285, 20181020. https://doi.org/10.1098/rspb.2018.1020.
Toggweiler, J.R., Russell, J.L., Carson, S.R., 2006. Midlatitude westerlies, atmospheric CO_2, and climate change during the ice ages. Paleoceanography 21. https://doi.org/10.1029/2005PA001154.
Towhidi, A., Seberifar, T., Dirandeh, E., 2011. Nutritive value of some herbage for dromedary camels in the central arid zone of Iran. Trop. Anim. Health Prod. 43, 617–622.
Trayler, R.B., Kohn, M.J., 2017. Tooth enamel maturation reequilibrates oxygen isotope compositions and supports simple sampling methods. Geochim. Cosmochim. Acta 198, 32–47. https://doi.org/10.1016/j.gca.2016.10.023.
Trayler, R.B., Dundas, R.G., Fox-Dobbs, K., Van De Water, P.K., 2015. Inland California during the Pleistocene—megafaunal stable isotope records reveal new paleoecological and paleoenvironmental insights. Palaeogeogr. Palaeoclimatol. Palaeoecol. 437, 132–140. https://doi.org/10.1016/j.palaeo.2015.07.034.
van Vuren, D., 1984. Summer diets of bison and cattle in southern Utah. J. Range Manag. 37, 260–261.
Vetter, L., 2007. Paleoecology of Pleistocene Megafauna in Southern Nevada, USA: Isotope Evidence for Browsing on Halophytic Plants. MS thesis. University of Nevada, Las Vegas, Las Vegas, NV, Geoscience.
Wagner, J.D.M., Cole, J.E., Beck, J.W., Patchett, P.J., Henderson, G.M., Barnett, H.R., 2010. Moisture variability in the southwestern United States linked to abrupt glacial climate change. Nat. Geosci. 3, 110–113.
Waelbroeck, C., Labeyrie, L., Michel, E., Duplessy, J.C., McManus, J.F., Lambeck, K., Balbon, E., Labracherie, M., 2002. Sea-level and deep water temperature changes derived from benthic foraminifera isotopic records. Quat. Sci. Rev. 21, 295–305. https://doi.org/10.1016/S0277-3791(01)00101-9.
Webb, R.H., Murov, M.B., Esque, T.C., Boyer, D.E., DeFalco, L.A., Haines, D.F.,

Oldershaw, D., Scoles, S.J., Thomas, K.A., Blainey, J.B., Medica, P.A., 2003. Perennial Vegetation Data from Permanent Plots on the Nevada Test Site, Nye County, Nevada, Open-File Report. United States Geological Survey, p. 251.

Williams, T.R., Bedinger, M.S., 1983. Selected Geologic and Hydrologic Characteristics of the Basin and Range Province, Western United States – Pleistocene Lakes and Marshes. United States Geological Survey Open-File Report, pp. 83–751. https://doi.org/10.3133/ofr83751.

Wynn, J.G., Bird, M.I., 2007. C4-derived soil organic carbon decomposes faster than its C3 counterpart in mixed C3/C4 soils. Global Change Biol. 13, 1–12.

Yann, L.T., DeSantis, L.R.G., Koch, P.L., Lundelius, E.L., 2016. Dietary ecology of Pleistocene camelids: influences of climate, environment, and sympatric taxa. Palaeogeogr. Palaeoclimatol. Palaeoecol. 461, 389–400. https://doi.org/10.1016/j.palaeo.2016.08.036.